ACS OMEGA

Open Access

http://pubs.acs.org/journal/acsodf

Article

Screening of α-Glucosidase Inhibitors in *Cichorium glandulosum* Boiss. et Huet Extracts and Study of Interaction Mechanisms

Adalaiti Abudurexiti,[⊥] Abliz Abdurahman,[⊥] Rui Zhang, Yewei Zhong, Yi Lei, Shuwen Qi, Wenhui Hou, and Xiaoli Ma*

Cite This: *ACS Omega* 2024, 9, 19401−19417

Read Online

ACCESS | Metrics & More | Article Recommendations | Supporting Information

ABSTRACT: *Cichorium glandulosum* Boiss. et Huet (*CGB*) extract has an α-glucosidase inhibitory effect (IC_{50} = 59.34 ± 0.07 μg/mL, positive control drug acarbose IC_{50} = 126.1 ± 0.02 μg/mL), but the precise enzyme inhibitors implicated in this process are not known. The screening of α-glucosidase inhibitors in CGB extracts was conducted by bioaffinity ultrafiltration, and six potential inhibitors (quercetin, lactucin, 3-O-methylquercetin, hyperoside, lactucopicrin, and isochlorogenic acid B) were screened as the precise inhibitors. The binding rate calculations and evaluation of enzyme inhibitory effects showed that lactucin and lactucopicrin exhibited the greatest inhibitory activities. Next, the inhibiting effects of the active components of *CGB*, lactucin and lactucopicrin, on α-glucosidase and their mechanisms were investigated through α-glucosidase activity assay, enzyme kinetics, multispectral analysis, and molecular docking simulation. The findings demonstrated that lactucin (IC_{50} = 52.76 ± 0.21 μM) and lactucopicrin (IC_{50} = 17.71 ± 0.64 μM) exhibited more inhibitory effects on α-glucosidase in comparison to acarbose (positive drug, IC_{50} = 195.2 ± 0.30 μM). Enzyme kinetic research revealed that lactucin inhibits α-glucosidase through a noncompetitive inhibition mechanism, while lactucopicrin inhibits it through a competitive inhibition mechanism. The fluorescence results suggested that lactucin and lactucopicrin effectively reduce the fluorescence of α-glucosidase by creating lactucin-α-glucosidase and lactucopicrin-α-glucosidase complexes through static quenching. Furthermore, the circular dichroism (CD) and Fourier transform infrared spectroscopy (FT-IR) analyses revealed that the interaction between lactucin or lactucopicrin and α-glucosidase resulted in a modification of the α-glucosidase's conformation. The findings from molecular docking and molecular dynamics simulations offer further confirmation that lactucopicrin has a robust binding affinity for certain residues located within the active cavity of α-glucosidase. Furthermore, it has a greater affinity for α-glucosidase compared to lactucin. The results validate the suppressive impact of lactucin and lactucopicrin on α-glucosidase and elucidate their underlying processes. Additionally, they serve as a foundation for the structural alteration of sesquiterpene derived from CGB, with the intention of using it for the management of diabetic mellitus.

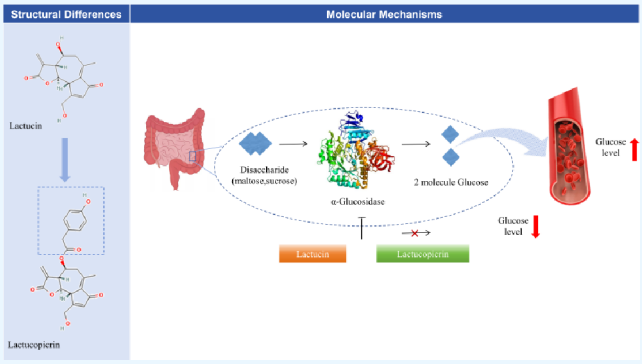

1. INTROUCTION

With people's living standards constantly rising and food patterns drastically shifting, diabetes has emerged as a highly frequent chronic ailment on a global scale. It is well-known that postprandial hyperglycemia is critical in developing diabetes (especially type 2 diabetes).[1] α-glucosidase inhibitors have been identified as a viable option for managing type 2 diabetes mellitus due to their ability to slow carbohydrate digestion and decrease the absorption of monosaccharides. This is due to their ability to maintain a stable blood glucose level within tolerable limits.[2] Therefore, one of the most important ways to stop diabetes from developing is to reduce postprandial hyperglycemia.[3,4] α-Glucosidase is found in a wide range of organisms.[5] The enzyme hydrolyzes carbohydrates in the digestive system to produce absorbable glucose.[6] Thus, inhibiting α-glucosidase can regulate the release of glucose and prevent postprandial hyperglycemia.[7] Currently, certain inhibitors, including acarbose and voglibose, are frequently used in clinical settings to help patients control their blood glucose levels. However, these drugs frequently result in gastrointestinal side effects, like bloating, diarrhea, and stomach pain.[8,9] Thus, the identification of α-glucosidase inhibitors from natural sources, including food matrices, is advantageous for the creation of novel antidiabetic medications.[10] The discovery of natural products has been widely

Received: January 21, 2024
Revised: March 20, 2024
Accepted: March 22, 2024
Published: April 18, 2024

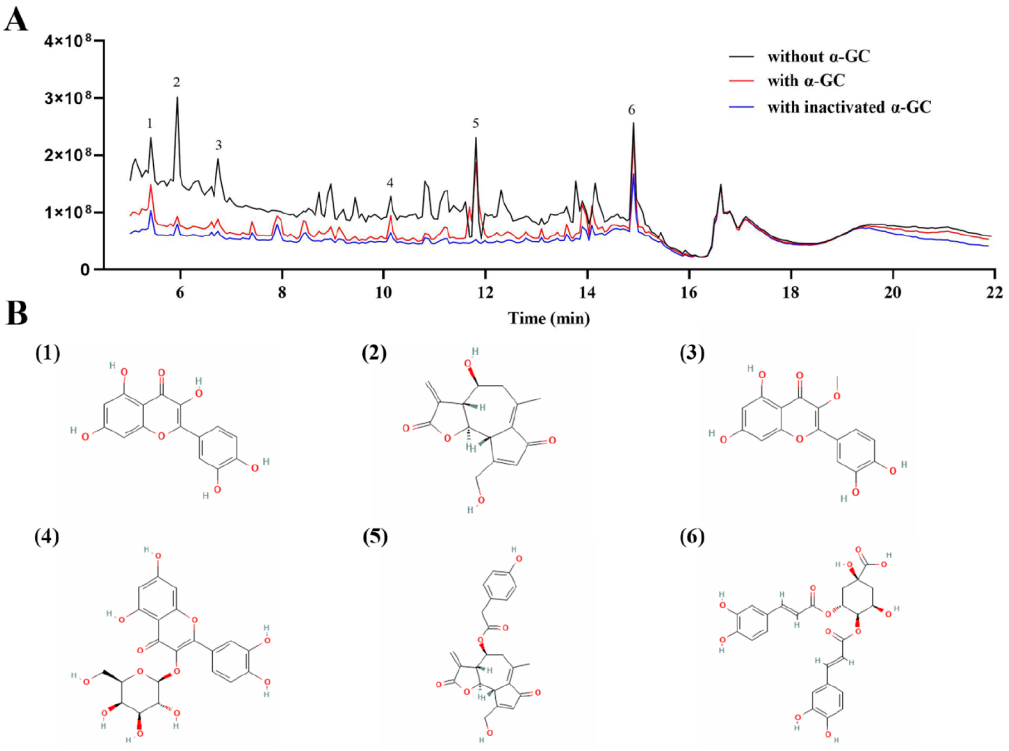

Figure 1. (A) UPLC−Q-TOF−MS/MS of chemical components in *CGB* obtained by affinity ultrafiltration, solid black, blue, and red lines represent the UPLC total ion peak profiles of *CGB* without α-glucosidase, with inactivated α-glucosidase, and with activated α-glucosidase, respectively; (B) identification of the chemical structures of compounds 1−6 in *CGB*.

accepted as potential, high-quality chemical libraries for screening drug candidates due to their unrivaled chemical diversity and biological relevance.[11]

Cichorium glandulosum Boiss. et Huet (*CGB*) is derived from the dried above-ground parts or roots of *CGB*, family *Asteraceae*, a multipurpose plant that is used as a vegetable, coffee companion, and folk medicine in China. *CGB* contains flavonoids, coumarins, sesquiterpenes, polysaccharides, and trace elements that cleanse the liver and gallbladder, strengthen the stomach, eliminate food, act as diuretic, and reduce swelling. It is used to treat damp-heat and jaundice, stomach pains with little food, and edema with little urine. *CGB* is cultivated more in Europe and other places as a kind of health-care vegetable, attracting much attention in foreign countries.[12] Pharmacological studies have shown that *CGB* has pharmacological effects, such as lowering blood sugar and regulating blood lipids.[13] *CGB* plant has been proven to inhibit α-glucosidase activity, which can control blood sugar more strictly.[14−16]*CGB* extracts are rich in sesquiterpenoids[17] and have received increasing attention for their antidiabetic properties. This study aimed to search for natural active ingredients in *CGB* with hypoglycemic effects. Due to the complexity of the chemical composition of *CGB*, the content of some components varies, some components have low content, and there is a synergistic effect of multiple components, a multitarget therapy phenomena.[18] The phenomenon of multitargeted therapy exists. So far, there are limited studies on the antidiabetic effect of *CGB*, and even fewer studies on its hypoglycemic effect. Conventional bioactive component screening procedures necessitate labor-intensive and time-consuming extraction, separation, and purification processes. Furthermore, common extracts such acidic hydrolases often result in the loss of phenolic compounds and even the production of furfural and its byproducts.[19] In contrast, the extremely sensitive and easy-to-use affinity ultrafiltration approach in conjunction with mass spectrometry.[20,21] It has been effectively utilized for screening novel bioactive ligands from complex compounds using affinity ultrafiltration.[22] For example, the study employed bioaffinity ultrafiltration coupled with HPLC−ESI−Q-TOF−MS/MS technology to identify seven compounds with α-glucosidase binding activity in the extracts of *Cerasus humilis* (Bge.) Sok. leaf-tea[23] and guava leaf-tea[24] to screen for potential α-glucosidase inhibitors. The purpose was to identify possible α-glucosidase inhibitors.

Hence, the current work focused on identifying the active components in the CGB by targeting certain biological markers. The mechanism of the conformational interaction between the active components in *CGB* to inhibit α-glucosidase in vitro was investigated using several techniques including enzyme kinetics, fluorescence spectroscopy, CD, UV spectroscopy, FT-IR, molecular docking, and molecular dynamics. This study offers a theoretical foundation for the development of hypoglycemic components in *CGB*. It also provides valuable information for enhancing the utilization of *CGB* for human health. This information can serve as a theoretical reference for the development of functional food components aimed at preventing and treating type 2 diabetes mellitus.

2. RESULTS AND DISCUSSION

2.1. Results of Inhibitory Activity Assay. Both the *CGB* extract and acarbose demonstrated strong enzyme inhibition in a manner that depended on the concentration. The IC_{50} values of the *CGB* extract and acarbose on α-glucosidase were 59.34 $\pm$ 0.07 and 126.1 $\pm$ 0.03 mg/mL, respectively, which showed that the inhibitory effect of *CGB* extract on α-glucosidase was

https://doi.org/10.1021/acsomega.4c00699
ACS Omega 2024, 9, 19401−19417

Table 1. Identification of Potential Active Ingredients in *CGB* Extracts Using UPLC−Q-TOF−MS/MS and their IC_{50} Values

peak no.	t_R (min)	m/z $[M-H]^-$ calculated	m/z $[M-H]^-$ measured	add ion $[MCOOH]^-$	error (ppm)	MS/MS (m/z)	molecular formula	identification	AD (%)	IC_{50} value (μM)
1	5.41	302.04265	302.0422	−H	−1.3	301.035	$C_{15}H_{10}O_7$	Quercetin	12.4	814.26±0.33
2	5.93	276.09977	276.0993	−H, +HCOO	−1.5	275.0921	$C_{15}H_{16}O_5$	Lactucin	51.2	52.76±0.21
3	6.74	316.0583	316.0565	−H	−5.6	315.0493	$C_{16}H_{12}O_7$	3-O-Methylquercetin	17.2	436.35±0.01
4	10.12	464.09548	464.0932	+HCOO	−4.5	509.0914	$C_{21}H_{20}O_{12}$	Hyperoside	23.4	1072.42±0.54
5	11.81	410.13655	410.1393	+HCOO	5.9	455.1375	$C_{23}H_{22}O_7$	Lactucopicrin	57.8	17.71±0.64
6	14.89	516.12678	516.1239	+HCOO	−5.2	561.1221	$C_{25}H_{24}O_{12}$	Isochlorogenic Acid B	13.5	497.62±0.2

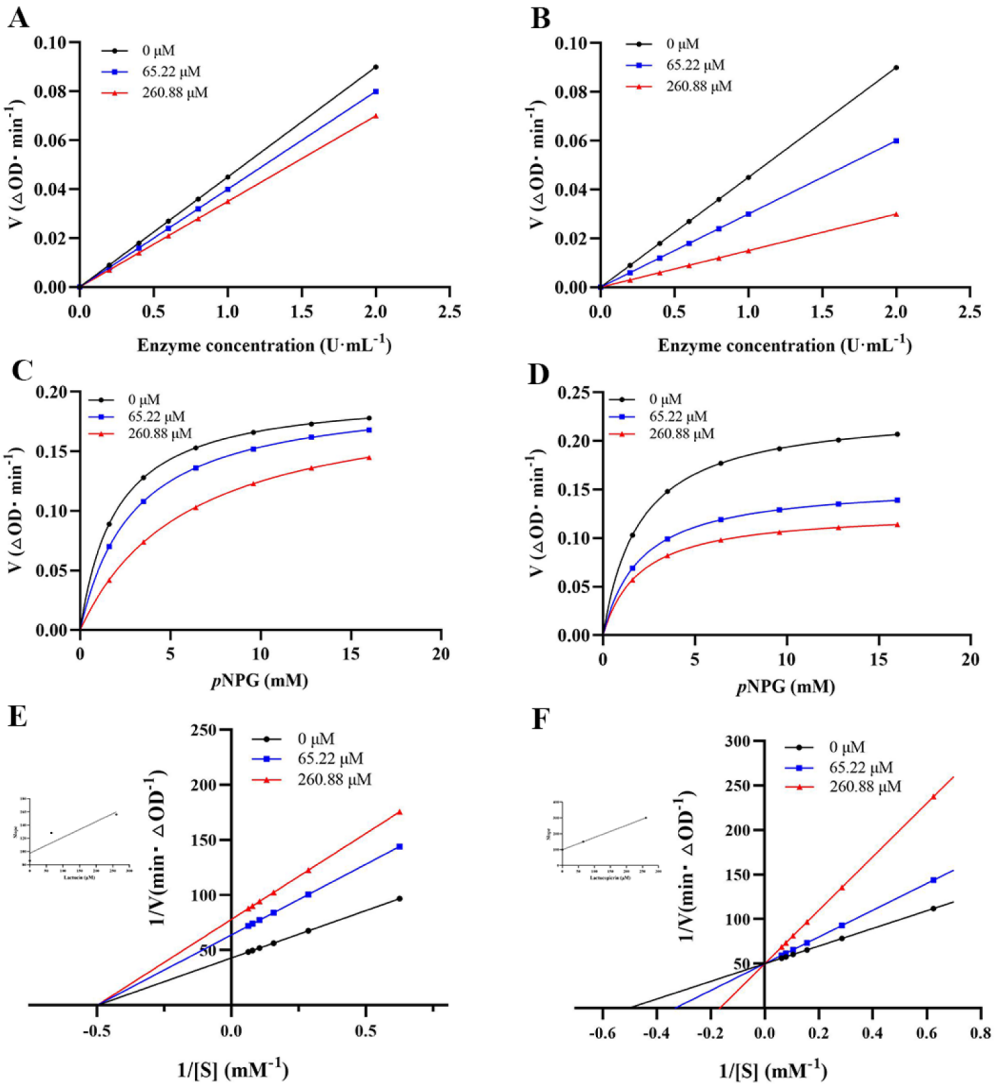

Figure 2. Michaelis−Menten and Lineweaver−Burk plots of enzyme kinetic studies of lactucin (A, C, E) and lactucopicrin (B, D, F) on α-glucosidase. The concentrations of lactucin and lactucopicrin in the reaction were 0, 26.09, and 65.22 μM.

higher than acarbose. The relatively low IC_{50} values suggest that the *CGB* extract has potential hypoglycemic effects. In conclusion, the *CGB* extract has an excellent inhibitory effect on α-glucosidase and can control postprandial hyperglycemia.

2.2. Screening and Characterization of Potential α-Glucosidase Inhibitors. To identify α-glucosidase inhibitors, the affinity ultrafiltration UPLC−Q-TOF−MS/MS coupling technique was used to screen and characterize α-glucosidase inhibitors in *CGB* extracts. After α-glucosidase incubation and ultrafiltration membrane retention, methanol was added to release the active compounds bound to α-glucosidase, which were further analyzed and recognized using UPLC−Q-TOF−MS/MS.

Figure 1 illustrates the presence of six prominent peaks in the chromatogram (Figure 1A). The screening results indicated a reduction in the peak areas of the six chromatographic peaks, implying that the components of these peaks may interact with α-glucosidase and have the potential to

https://doi.org/10.1021/acsomega.4c00699
ACS Omega 2024, 9, 19401−19417

Table 2. Analysis of the Kinetic Parameters of α-Glucosidase with and Without the Presence of Lactucin and Lactucopicrin

system	concentration of inhibitor (μM)	v_{max} (mM/min)	K_m (mM)	K_i (mM)	type
α-glucosidase−lactucin	0	0.023	2.01	87.59	noncompetitive
	26.09	0.016			
	65.22	0.013			
α-glucosidase−lactucopicrin	0	0.022	1.98	27.82	competitive
	26.09		3.02		
	65.22		5.96		

decrease its activity as α-glucosidase inhibitors. The six peaks (1−6) were recognized as ligands for α-glucosidase. The reduction in peak area for each inhibitor in the unbound percentage of the incubated complexes as compared to the control indicates the binding affinity of the inhibitor for α-glucosidase. Peak 5 had the greatest affinity at 57.8%, followed by peak 2 at 51.2%, peak 4 at 23.4%, peak 3 at 17.2%, peak 6 at 13.5%, and peak 1 at 12.4%. Nevertheless, due to the absence of a direct positive link between the affinity degree (AD) values and the severity of inhibition, it remains uncertain whether the aforementioned α-glucosidase ligands caused inhibition.

The negative ion mode facilitates the differentiation between molecular ions and paramolecular ions more effectively than the positive ion mode. The identification of active chemicals involved the comparison of fragment types and structures with references or public databases, such as ChemSpider, PubChem, and Massbank. The information described in Table 1 includes retention times (t_R), predicted and measured molecular masses, additional ions, mass errors, MS/MS fragment ions, molecular formulas, identification results, and references. Figure 1 displays the chemical structures of the possible α-glucosidase inhibitors in *CGB*. After careful analysis, six chemicals were ultimately shown to be present. These compounds were identified as quercetin (1), lactucin (2), 3-O-methylquercetin (3), hyperoside (4), lactucopicrin (5), and isochlorogenic acid B (6). This information is depicted in Figure 1B and Table 1. The components that were found consist of two flavonols (compounds 1 and 3), two sesquiterpene lactone monomers (compounds 2 and 5), a flavonol glycoside (compound 4), and a phenylpropanoid (compound 6). The identification of these six components as possible α-glucosidase inhibitors of the *CGB* extract is a novel finding.

2.3. Identification of Compounds with α-Glucosidase Inhibitory Activity. Compounds 1−6 isolated from *CGB* extract showed different degrees of inhibition of α-glucosidase with IC_{50} values of quercetin (IC_{50} = 814.26 ± 0.33 μM), lactucin (IC_{50} = 52.76 ± 0.2 μM), 3-O-methylquercetin (IC_{50} = 436.35 ± 0.01 μM), hyperoside (IC_{50} = 1072.42 ± 0.54 μM), lactucopicrin (IC_{50} = 17.71 ± 0.64 μM), and isochlorogenic acid B (IC_{50} = 497.62 ± 0.2 μM). The order of magnitude of inhibitory activity was lactucopicrin > lactucin >3-O-methylquercetin > isochlorogenic acid B > quercetin > hyperoside. The inhibitory activity exhibited superior efficacy compared to acarbose, which served as the positive control medication with an IC_{50} value of 195.2 ± 0.3 μM. The inhibition curves of α-glucosidase by the six compounds are shown in Figure S5. The compounds were lactucin and lactucopicrin, indicating that these two compounds had good inhibitory activity. Comparing the inhibitory activities of lactucin and lactucopicrin, we found that lactucopicrin has a higher α-glucosidase inhibitory activity. The structure and inhibitory activity of lactucin was enhanced after the addition of *p*-hydroxyphenyl acetic acid for esterification with the 2-position hydroxyl group, so the present work is to conduct a conformational relationship study on the compounds, which have a very similar structure but with different inhibitory activities against the enzyme and to find out the structure of the compounds after adding the group to their inhibitory activity. Therefore, we investigated the conformational relationship of these compounds with similar structures but different enzyme inhibitory activities and found out the added groups' effect on the compounds' inhibitor-enzyme reaction system.

2.4. Enzyme Kinetic Studies. The curves depicting the relationship between the reaction rate and α-glucosidase concentration were analyzed to assess the extent of inhibition reversibility caused by lactucin (Figure 2A) and lactucopicrin (Figure 2B). Two compounds were represented by three straight lines each, intersecting at the origin of the coordinate axes. The gradients diminished as the concentrations of lactucin or lactucopicrin increased, indicating that the interaction between the two chemicals and the enzyme can be reversed. Furthermore, the reversible inhibition demonstrated the occurrence of noncovalent intermolecular contacts between lactucin or lactucopicrin and α-glucosidase, leading to a reduction in enzyme activity.

The hydrolysis rate of substrates by α-glucosidase was measured both with and without lactucin (Figure 2C) and lactucopicrin (Figure 2D). K_m and v_{max} were determined by nonlinear regression analysis using GraphPad Prism 9 software. The specific values are given in Table 2. Figure 2E,F displays the findings of the enzyme kinetic experiments. The *x*-axis represents the substrate concentration, while the *y*-axis represents the reaction rate.

The K_m value for Lactucin remained consistent, whereas the v_{max} value declined with an increasing lactucin concentration (Figure 2E). This suggests that lactucin acts as a noncompetitive inhibitor. The noncompetitive inhibitors exhibited a high affinity for both the free enzyme and the enzyme−substrate complexes, as well as other subsequent compounds. This resulted in the formation of EI-complexes and ESI-complexes.

The longitudinal intercept ($1/v_{max}$) of lactucopicrin remained consistent as the quantities of lactucopicrin increased. Nevertheless, the slope (K_m/v_{max}) and the cross-axis intercept ($-1/K_m$) exhibited changes in response to the concentration of lactucopicrin (Figure 2F). This indicates that lactucopicrin triggers a competitive inhibition mechanism of α-glucosidase, where it competes with the substrate for the available enzyme molecules, resulting in the formation of enzyme−inhibitor complexes.[25]

K_m^{app}, $1/v_{max}^{app}$, or the quadratic plot of slope vs $[I]$ are shown in the upper left corner of the corresponding plots of Figure 2E,F. The K_i values were obtained using the formulas specified above, depending on the kind of inhibition. The findings are

https://doi.org/10.1021/acsomega.4c00699
ACS Omega 2024, 9, 19401−19417

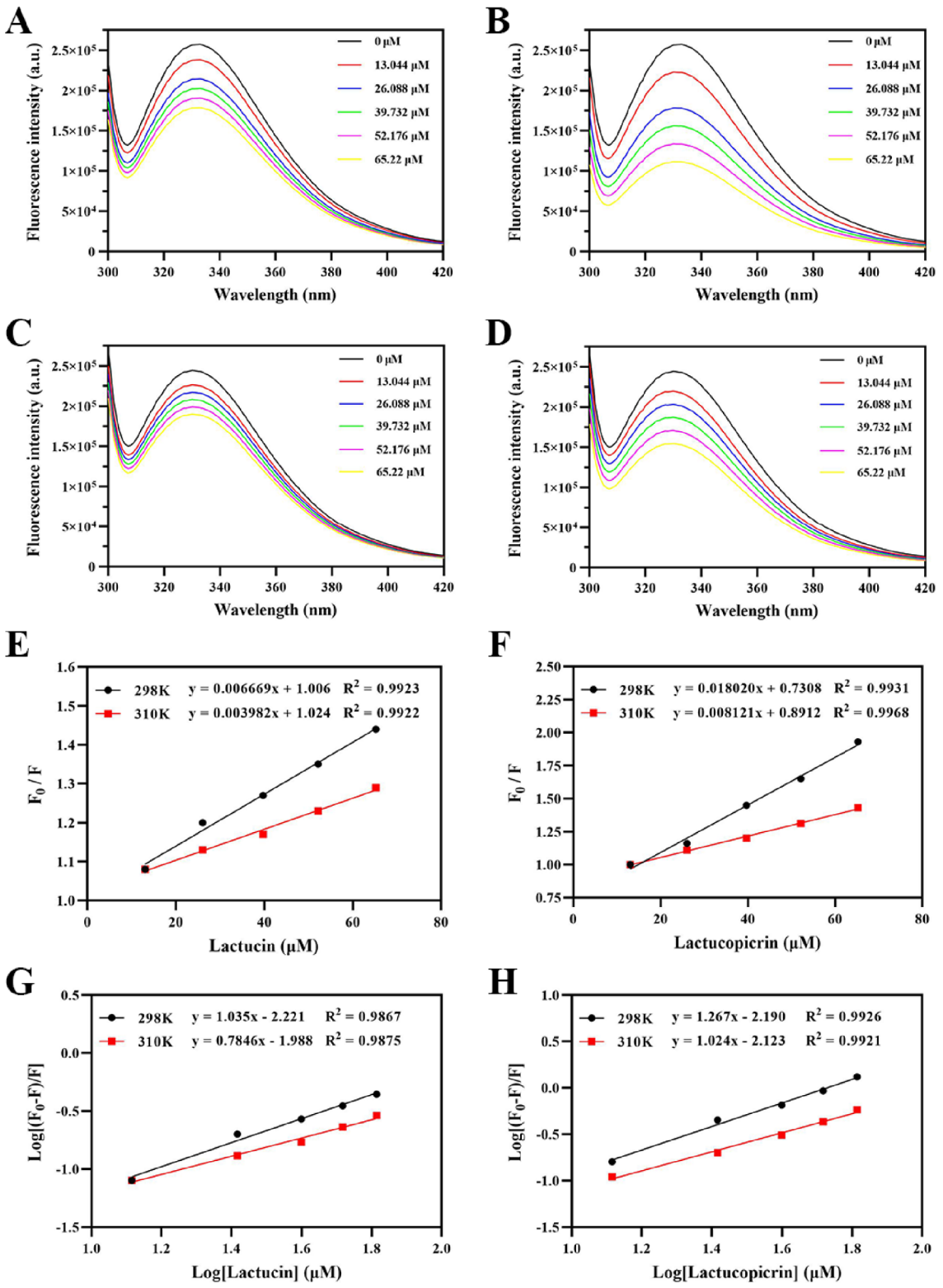

Figure 3. Fluorescence spectra of α-glucosidase in the presence of different concentrations of lactucin (A) and lactucopicrin (B) at 298 K; fluorescence spectra of α-glucosidase in the presence of different concentrations of lactucin (C) and lactucopicrin (D) at 310 K; Stern−Volmer plots; Stern−Volmer plots of fluorescence quenching of lactucin (E) and lactucopicrin (F); modified Stern−Volmer plots of fluorescence quenching of lactucin (G) and lactucopicrin (H) against α-glucosidase. $C_{\alpha\text{-glucosidase}}$ = 2 U/mL, C_{lactucin}=$C_{\text{lactucopicrin}}$ = 0, 13.044, 26.088, 39.732, 52.176, and 65.22 μM.

listed in Table 2. K_i is the equilibrium dissociation constant that characterizes the balance between the binary complex formed by the free enzyme and the inhibitor. A lower K_i value indicates a greater binding affinity between the inhibitor and the enzyme. The findings demonstrated that the K_i value of lactucopicrin was comparatively lower than that of lactucin, suggesting that lactucopicrin exhibited a greater inhibitory effect on α-glucosidase than lactucin.

https://doi.org/10.1021/acsomega.4c00699
ACS Omega 2024, 9, 19401−19417

Table 3. Quenching Parameters of α-Glucosidase by Lactucin and Lactucopicrin at Different Temperatures

system	T (K)	K_{sv} (L mol^{-1})	R^2	K_q (L mol^{-1}s^{-1})	quenching type
α-glucosidase−lactucin	298	6.63×10^3	0.9923	6.63×10^{11}	static quenching mechanism
	310	3.89×10^3	0.9922	3.89×10^{11}	
α-glucosidase−lactucopicrin	298	2.47×10^4	0.9931	2.47×10^{12}	static quenching mechanism
	310	9.11×10^3	0.9968	9.11×10^{11}	

Table 4. Thermodynamic Parameters of the Lactucin/Lactucopicrin−α-Glucosidase System

system	T (K)	K_a (L mol^{-1})	n	R^2	$\Delta H°$ (kJ·mol^{-1})	$\Delta S°$ (J·mol·K^{-1})	$\Delta G°$ (kJ·mol^{-1})
α-glucosidase−lactucin	298	6.01×10^3	1.04	0.9867	34.48	188.05	−21.56
	310	1.03×10^4	0.78	0.9875			−23.82
α-glucosidase−lactucopicrin	298	6.46×10^3	1.27	0.9926	9.81	105.86	−21.74
	310	7.53×10^3	1.02	0.9921			−23.01

Despite the close structural similarity between lactucin and lactucopicrin, they exhibit distinct inhibitory actions on α-glucosidase, indicating notable distinctions between them. Lactucin mostly exhibits noncompetitive inhibition toward α-glucosidase. On the other hand, lactucopicrin mostly inhibits α-glucosidase by competitive inhibition, which is mainly due to the structural distinction between lactucin and lactucopicrin.

2.5. Analysis of Fluorescence Quenching. In order to have a deeper comprehension of the inhibitory mechanism of lactucin and lactucopicrin on α-glucosidase, fluorescence spectroscopy was employed to investigate the impact of these two chemicals on the fluorescence of α-glucosidase at two different temperatures, namely, 298 and 310 K. Figure 3 demonstrates that the fluorescence intensity of α-glucosidase reduced when the concentrations of lactucin (Figure 3A) and lactucopicrin (Figure 3B) increased from 0 to 65.22 μM at 298 K. This suggests that the two compounds have the ability to interact with α-glucosidase. At a temperature of 310 K, the fluorescence intensity of α-glucosidase reduced when the concentration of lactucin (Figure 3C) and lactucopicrin (Figure 3D) increased from 0 to 65.22 μM. This suggests that the two compounds have the ability to interact with α-glucosidase. Under the same temperature conditions, the suppressive impact of lactucin on α-glucosidase fluorescence was considerably less pronounced compared to that of lactucopicrin. Furthermore, the compound's ability to suppress the enzyme was shown to differ at various temperatures, with a notably poorer suppression observed at 310 K compared to 298 K. The suppressive impact of lactucin on the fluorescence of α-glucosidase was considerably less pronounced compared to that of lactucopicrin. The red-shift caused by lactucin was less pronounced compared to the red-shift caused by lactucopicrin, indicating that the structural alteration of α-glucosidase by lactucopicrin was not significantly less potent than that induced by lactucopicrin.[26,27]

Quenching mechanisms can be broadly classified as static quenching, dynamic quenching, or a combination of both.[28] Static quenching involves the formation of a basal complex between the fluorophore and the quenching agent, while dynamic quenching suggests a collision between the two. To clarify the process by which lactucin and lactucopicrin inhibit enzyme activity, the fluorescence data were analyzed using the Stern−Volmer equation:[29]

$$F_0/F = K_{sv}[Q] + 1 = K_q\tau_0[Q]$$

where $[Q]$ represents the concentration of the component, F_0 represents the fluorescence intensity of a solution containing free-α-glucosidase, F represents the fluorescence intensity of α-glucosidase at various doses of inhibitors, and K_q represents the rate constant at which the biomolecule is quenched. The typical fluorescence lifetime of α-glucosidase in pure solution is τ_0, which is equal to 1×10^{-8} s.

An analysis was conducted on the association between K_{sv} and the temperature (T). Figure 3E,F demonstrates a negative correlation between lactucin and lactucopicrin with T vs K_{sv}. In addition, as shown in Table 3, the K_q values of lactucin and lactucopicrin were one or two orders of magnitude greater than the maximum scattering collision quenching constant (2.0×10^{10} L·mol^{-1}·s^{-1}). The findings demonstrated that lactucin and lactucopicrin caused a decrease in the fluorescence intensity of α-glucosidase by a process known as static quenching. The findings indicated that both chemicals had an effect on the fluorescence intensity of the enzyme through static quenching. Lactucopicrin is synthesized by incorporating a 2-(4-hydroxyphenyl) acetic acid moiety into the molecular framework of lactucin. The change had a minimal or negligible impact on the quenching mechanism of the compounds.

2.6. Binding Sites and Binding Constants. According to the following equation,[30] the binding sites (n) and binding constants (K_a) of lactucin or lactucopicrin with α-glucosidase were determined:

$$\log(F_0 - F)/F = n \log[Q] + \log K_a$$

As shown in Table 4, the results of the K_a values of lactucin and lactucopicrin indicate that the compounds have a high affinity for the enzyme. By comparing the K_a values of lactucin or lactucopicrin at the same temperature, the results indicate that the addition of a 2-(4-hydroxyphenyl) acetic acid group on the 2-position of lactucopicrin can increase the affinity of the molecule with α-glucosidase.

As can be seen from Figure 3G,H, as the temperature increases, the ability of lactucin-α-glucosidase and lactucopicrin-α-glucosidase to bind weakens.[31,32] Given that all n values are around 1, it may be inferred that there is only a single potential binding site for both substances on the enzyme. The data are shown in Table 4, where the K_a values increase with increasing temperature, and all data are within the range of 10^3 −10^4 L·mol^{-1}, indicating that the stability of α-glucosidase−lactucin and α-glucosidase−lactucopicrin complexes increases with increasing temperature and that lactucin and lactucopicrin have a high affinity for α-glucosidase. In addition, comparing the K_a values of lactucin and lactucopicrin, it was found that

https://doi.org/10.1021/acsomega.4c00699
ACS Omega 2024, 9, 19401−19417

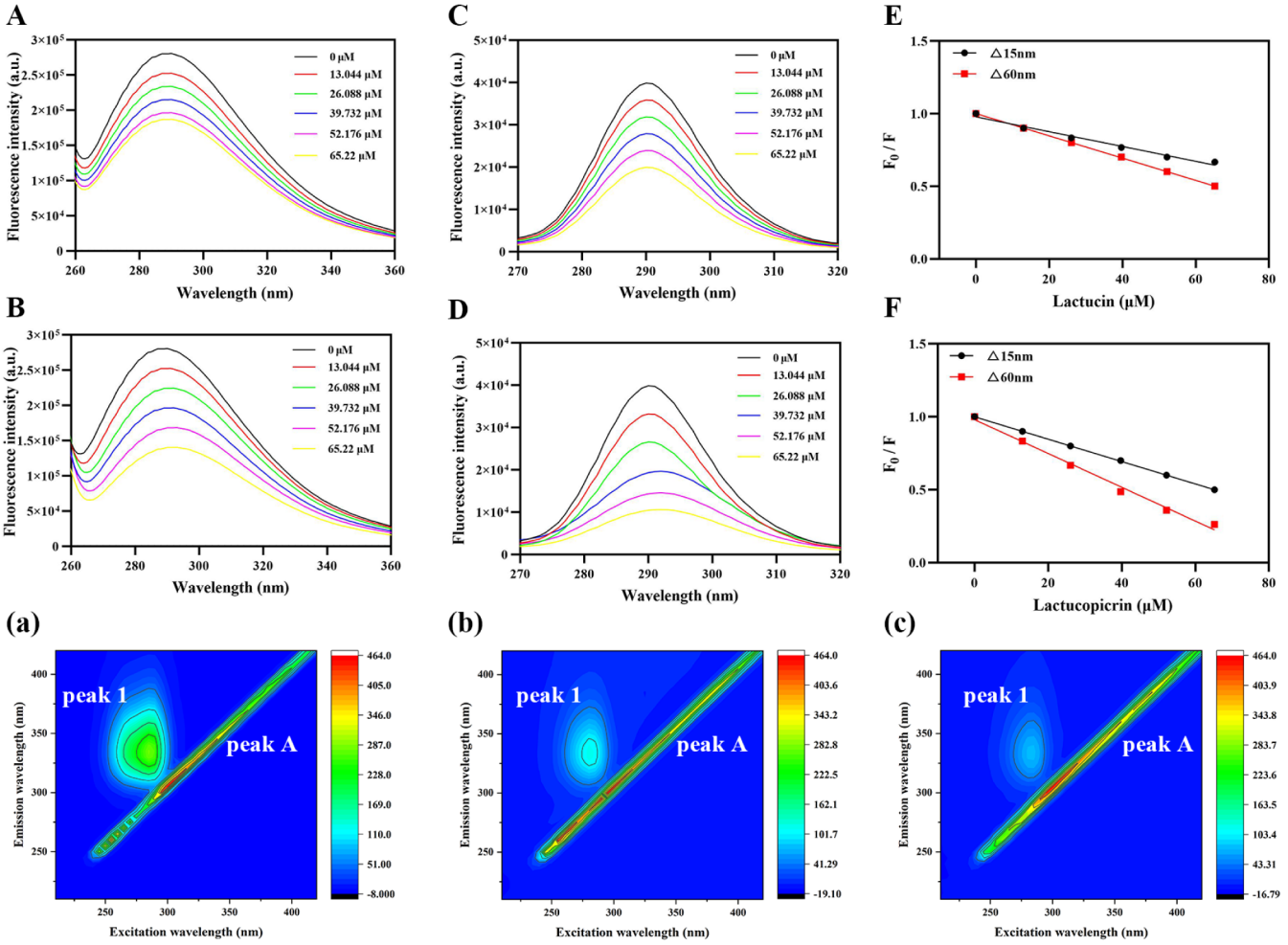

Figure 4. Synchronized fluorescence spectra of α -glucosidase with lactucin (A) and lactucopicrin (B) at $\Delta\lambda$ = 15 nm; synchronized fluorescence spectra of α-glucosidase with lactucin (C) and lactucopicrin (D) at $\Delta\lambda$ = 60 nm; plots of corresponding synchronized fluorescence quenching rates (RSFQ) will be for lactucin (E) and lactucopicrin (F), respectively; $C_{\alpha\text{-glucosidase}}$ = 2U/mL, C_{lactucin} = $C_{\text{lactucopicrin}}$ = 0, 13.044, 26.088, 39.732, 52.176, and 65.22 μM. 3D fluorescence spectra of free-α-glucosidase (a), lactucin−α-glucosidase complex (b), and lactucopicrin−α-glucosidase complex (c); $C_{\alpha\text{-glucosidase}}$ = 2U/mL, C_{lactucin} = $C_{\text{lactucopicrin}}$ = 65.22 μM.

lactucin had a higher affinity for α-glucosidase than lactucopicrin.

2.7. Thermodynamic Changes and Bonding Analysis. Protein−ligand complexes are stabilized via hydrophobic interactions, hydrogen bonds, van der Waals forces, and electrostatic binding.[33] Calculating thermodynamic parameters is essential to differentiate the binding force of lactucin or lactucopicrin to α-glucosidase. Small molecules and proteins engage in interactions through electrostatic, van der Waals, and hydrophobic forces, as well as hydrogen bonding. When the temperature change is minimal, we can treat ΔH° as a constant.[34] The thermodynamic parameters of the interaction between the chemical and α-glucosidase can be determined by performing parameter calculations using the Van't Hoff and Gibbs−Helmholtz equations:[35]

$$\log K_a = -\frac{1}{2.303RT}(\Delta H^\circ - T\Delta S^\circ)$$

$$\Delta G^\circ = \Delta H^\circ - T\Delta S^\circ$$

$$\Delta G^\circ = -RT \ln K_a$$

$$\Delta S^\circ = (\Delta H^\circ - \Delta G^\circ)/T$$

$$\ln\left(\frac{K_2}{K_1}\right) = \left(\frac{1}{T_1} - \frac{1}{T_2}\right)\frac{\Delta H^\circ}{R}$$

where K_a denotes the binding constant of α-glucosidase to the compound at different temperatures, ΔH° denotes the associated enthalpy change, ΔG° denotes the associated change in the free Gibbs energy, ΔS° represents the alteration in entropy linked to the reaction, and R = 8.314 J·mol^{-1}·K^{-1}.

The positive values of ΔH° and ΔS° for lactucin and lactucopicrin suggest that hydrophobicity is the main factor influencing the binding process of these compounds to α-glucosidase.[36] The outcomes of ΔG°. Furthermore, the negative ΔG° values suggest that there is a spontaneous interaction between α-glucosidase and lactucin or lactucopicrin.[34] The similar values of ΔG°, ΔH°, and ΔS° for both lactucin and lactucopicrin indicate that the inclusion of the 2-(4-hydroxyphenyl) acetate group has a minimal impact on the driving force for complex formation.

2.8. Synchronized Fluorescence Studies. Synchronous fluorescence spectroscopy is essential for studying structural and microenvironmental changes near protein chromophores. According to the theory proposed by Fuller and Miller, when

https://doi.org/10.1021/acsomega.4c00699
ACS Omega 2024, 9, 19401−19417

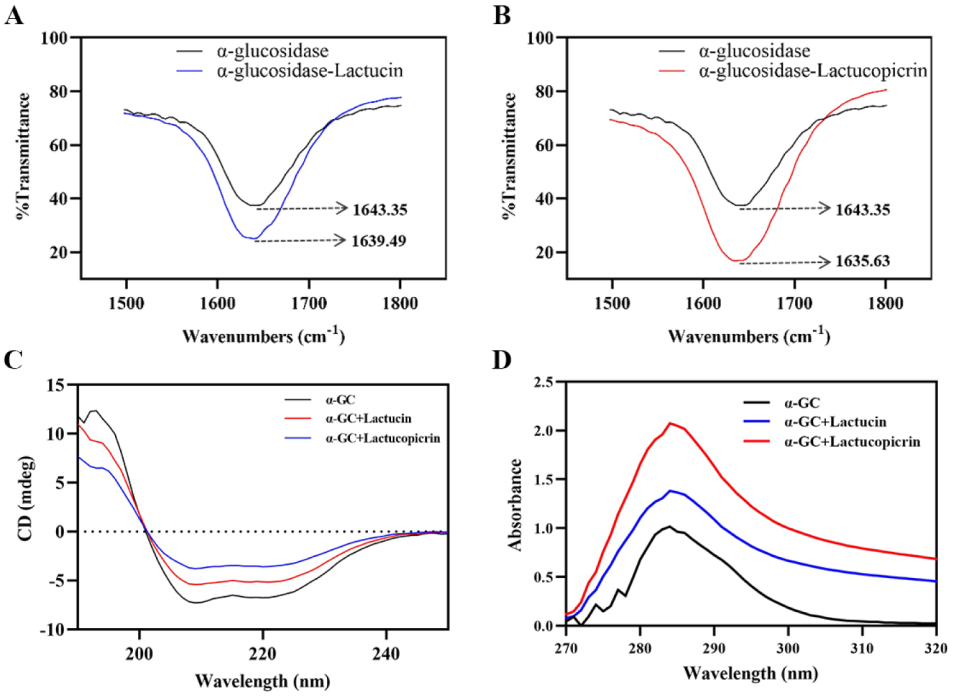

Figure 5. FT-IR spectra: A is the effect of lactucin on the amide I bond of α-glucosidase, and B is the effect of lactucopicrin on the amide I bond of α-glucosidase; C is the circular dichroism chromatogram: the effect of lactucin and lactucopicrin on α-glucosidase; and D is the UV spectra: the effect of lactucin and lactucopicrin on α-glucosidase. $C_{\alpha\text{-glucosidase}}$ = 2U/mL, C_{lactucin} = $C_{\text{lactucopicrin}}$ = 65.22 μM.

the wavelength interval ($\Delta\lambda$) is set at 15 and 60 nm, it provides specific information on the tyrosine (Tyr) and tryptophan (Trp) residues. The main fluorescent groups in glucosidase are Tyr and Trp.[37] A blue or red shift of the maximum absorption peak corresponds to an increase in the hydrophobicity and hydrophilicity of the microenvironment.[38] The shift in the highest absorption peak, either toward blue or red, indicates a change in the hydrophobicity and hydrophilicity of the microenvironment.

The fluorescence intensity of the peaks in Figure 4A,B ($\Delta\lambda$ = 15 nm) and Figure 4C,D ($\Delta\lambda$ = 60 nm) reduced notably when the amounts of lactucin and lactucopicrin increased. This indicates that the fluorescence quenching of α-glucosidase is linked to the Tyr and Trp residues.[39] In addition, with the increase in the concentration of lactucin (Figure 4A,C), only the absorption peak of the Trp residue was red-shifted from 288 to 290.5 nm, suggesting that lactucin only increased the polarity around the Trp residue in α-glucosidase and decreased its hydrophobicity. Meanwhile, after the addition of lactucopicrin (Figure 4B,D), the absorption peaks of Tyr and Trp residues exhibited a red-shift, moving from 288 to 292 nm and from 290 to 293.5 nm, respectively. This indicates that lactucopicrin has the ability to enhance the polarity of the microenvironments surrounding Tyr and Trp residues, while reducing the hydrophobic nature of these environments. Consequently, the solvent exposure of these two residues increased.[3] Lactucin and lactucopicrin hinder the activity of α-glucosidase by altering its structure. Lactucopicrin differs from lactucin in its interaction with Tyr and Trp residues, causing a change in the conformation of α-glucosidase. In contrast, lactucin interacts solely with Trp residues. Furthermore, the decline in $\Delta\lambda$ = 60 nm was considerably more resilient compared to $\Delta\lambda$ = 15 nm, as depicted in Figure 4E,F. This indicates that Trp residues have a considerable impact on fluorescence quenching in relation to Tyr residues.

2.9. 3D Fluorescence Analysis. Lactucin and lactucopicrin inhibit the function of α-glucosidase via modification of its molecular structure. Lactucopicrin has distinct interactions with Tyr and Trp residues, resulting in a modification of the α-glucosidase conformation, unlike lactucin. On the other hand, lactucin specifically interacts with Trp residues. In addition, the decrease in $\Delta\lambda$ = 60 nm showed greater durability in comparison to $\Delta\lambda$ = 15 nm, as illustrated in Figure 4E,F. Trp residues have a significant influence on fluorescence quenching compared to Tyr residues.[29] Furthermore, peak 1, which exhibits intense fluorescence, mostly represents the spectral characteristics of Trp and Tyr amino acid residues. Figure 4 demonstrates that the fluorescence intensity of peak 1 decreased by 59.82% following the introduction of lactucin into the α-glucosidase solution. By contrast, the addition of lactucopicrin resulted in a 72.11% decrease in the fluorescence intensity of peak 1.

The results showed that there were structural and microenvironmental changes that took place after the binding of lactucin or lactucopicrin to α-glucosidase. These findings were in line with the results obtained from a simultaneous fluorescence spectroscopy study. Furthermore, it was demonstrated that α-glucosidase had a greater affinity for lactucopicrin compared to lactucin. Additionally, the quenching abilities of lactucin and lactucopicrin differed due to the presence of the 2-(4-hydroxyphenyl) acetic acid group. This outcome is also in agreement with the findings of fluorescence quenching.

2.10. FT-IR Analysis. To evaluate the interaction between α-glucosidase and lactucin and lactucopicrin, FT-IR spectroscopy was used to further investigate the structural changes in α-glucosidase caused by these molecules.[40] Figure 5A,B demonstrates that there were no additional distinct peaks observed in the FT-IR spectra of the lactucin−α-glucosidase and lactucopicrin−α-glucosidase complexes. This indicates

https://doi.org/10.1021/acsomega.4c00699
ACS Omega 2024, 9, 19401−19417

that no new covalent bonds were formed during the interaction.

The FT-IR spectra of proteins often exhibit distinct peaks corresponding to the N−H stretching vibration (3300−2070 cm^{-1}), amide I band (1700−1600 cm^{-1}), amide II band (1550 cm^{-1}), and amide III band (1400−1200 cm^{-1}).[41] The characteristics of the peaks in the amide II band (1550 cm^{-1}) and amide III band (1400−1200 cm^{-1}) were determined. Nevertheless, the amide I band, which corresponds to the C−O stretching vibration, exhibits a higher degree of sensitivity toward alterations in the secondary structure of proteins compared to the other bands.[42] In order to further investigate the impact of the chemicals on α-glucosidase, the amide I band of the samples was analyzed by using FT-IR.

The amide I band peaks were seen at 1643.35 cm^{-1} (free α-glucosidase), 1639.49 cm^{-1} (lactucin−α-glucosidase), and 1635.63 cm^{-1} (lactucopicrin−α-glucosidase), as depicted in Figure 5A,B. The addition of lactucin caused a slight but significant shift in the peak position of the amide I band. Similarly, the peak position of the amide I band was significantly shifted after the addition of lactucopicrin. This suggests that both lactucin and lactucopicrin interacted with the amide I band in α-glucosidase, leading to a rearrangement of the hydrogen bonding pattern of the polypeptide carbonyl group.[42] The amide I band peaks were seen at 1643.35 cm^{-1} (free α-glucosidase), 1639.49 cm^{-1} (lactucin−α-glucosidase), and 1635.63 cm^{-1} (lactucopicrin−α-glucosidase), as shown in Figure 5A,B. The inclusion of lactucin resulted in a small yet noteworthy displacement in the peak location of the amide I band. Furthermore, the addition of lactucopicrin caused a considerable shift in the peak location of the amide I band. These findings indicate that both lactucin and lactucopicrin affected the amide I band in α-glucosidase, causing a reorganization of the hydrogen bonding pattern of the polypeptide carbonyl group.

2.11. CD Analysis. The CD spectra of α-glucosidase displayed two distinct negative peaks at around 208 and 220 nm, as depicted in Figure 5C. These peaks are indicative of the presence of an α-helical structure.[43] The study revealed that the CD spectrum intensity of α-glucosidase was notably diminished upon the introduction of the two inhibitors (lactucin and lactucopicrin). This suggests that the inhibitors' binding caused a modification in the spatial structure of α-glucosidase. Concurrently, the proportion of the secondary structure of α-glucosidase was ascertained, and the corresponding values are presented in Table 5. The findings indicated that the presence of lactucin led to a decrease in the proportion of α-helix content from 36.8% to 30.3%. Conversely, the proportion of the β-sheet content increased from 13.7% to 15.5%, and the proportion of β-turns increased from 21.0% to 21.3%. The percentage of random coil has risen from 28.5% to 32.9%.

Table 5. Secondary Structure Content of the three Samples at Room Temperature

systems	α-helix (%)	β-sheet (%)	β-turn (%)	random coil (%)
α-glucosidase	36.8	13.7	21.0	28.5
α-glucosidase−lactucin	30.3	15.5	21.3	32.9
α-glucosidase−lactucopicrin	23.7	20.8	24.4	31.1

Similarly, the binding of lactucopicrin to α-glucosidase resulted in a decrease in protein (α-helix from 36.8 to 23.7%; β-sheet from 13.7 to 20.8%; β-turns from 21.0 to 24.4%). The secondary structure of the random coil, which increased from 28.5 to 31.1%, was significantly changed. Overall, the findings suggest that the interaction between lactucin or lactucopicrin and α-glucosidase caused the enzyme to unfold and change its secondary structure. This, in turn, affected the binding of the enzyme to its substrate or hindered the formation of the active site, resulting in the inhibition of enzyme activity.[44] The results demonstrated that the interaction between lactucopicrin and α-glucosidase caused a notable alteration in the enzyme's secondary structure. This change was considerably more pronounced compared to the effect induced by lactucin. This disparity in the inhibitory activity against α-glucosidase between the two compounds may be attributed to this discrepancy in the structural impact.

2.12. UV Analysis. Figure 5D displays the UV absorption spectra of α-glucosidase both without any inhibitor and with the inclusion of either lactucin or lactucopicrin as inhibitors. In the presence of lactucin or lactucopicrin, the absorbance of the enzyme near 283 nm increased with a slight red shift, indicating that α-glucosidase interacts with lactucin or lactucopicrin to form an enzyme−inhibitor complex, which results in a conformational change of the enzyme.[45] The α-glucosidase enzyme formed a compound with either lactucin or lactucopicrin, which acted as inhibitors. This complex caused a change in the shape of the enzyme. Furthermore, the enzyme exhibited a more significant rise in absorbance and a greater red shift for lactucopicrin compared to lactucin. This outcome is also in line with the empirical findings of circular dichroism.

2.13. Molecular Docking. Molecular docking is a method used to visually represent and analyze the structural changes that occur in the interactions between receptors and ligands.[46] Figure 6 presents the most favorable docking outcomes for the interactions between lactucin or lactucopicrin and α-glucosidase, with binding energies of −5.6 and −7.2 kcal/mol, respectively. The binding of both drugs to α-glucosidase was investigated using the CDOCKER tool in Discovery Studio (Version 2.5). The molecular docking results of the lactucin−α-glucosidase system are illustrated in Figure 6A−C. The results indicated that lactucin was located within the active site of α-glucosidase, which was encompassed by ten specific amino acid residues: Arg-439, Asp-349, Glu-276, Asp-214, Phe-177, Leu-218, Ala-278, Phe-157, Phe-300, and Arg-312. Figure 6B illustrates the formation of a hydrogen bond between lactucin and amino acid residue Arg-439, at a distance of 2.9 Å. Furthermore, lactucin formed many interactions with certain amino acid residues (Glu-276, Phe-157, Phe-300, Ala-278) as depicted in Figure 6C. These bonds include carbon−hydrogen bonds, π−σ bonds, alkyl bonds, and π-alkyl bonds. Lactucin mostly interacts with the enzyme through hydrogen bonds, hydrophobic contacts, and van der Waals forces. This interaction hampers the binding between the substrate and α-glucosidase, resulting in a decrease in enzyme activity. The molecular docking results of the lactucopicrin−α-glucosidase system are depicted in Figure 6D−F. Lactucopicrin mostly interacted with specific amino acid residues of α-glucosidase, namely Arg-439, Asp-349, Glu-276, Asp-214, Phe-177, Leu-218, Ala-278, Phe-157, Phe-300, and Arg-312. Phe-157, Phe-300, and Arg-312 were in the proximity of each other. Arg-439 and Phe-157 established two hydrogen bonds with lactucopicrin, with distances of 3.3 and 2.8 Å, respectively. Furthermore,

https://doi.org/10.1021/acsomega.4c00699
ACS Omega 2024, 9, 19401−19417

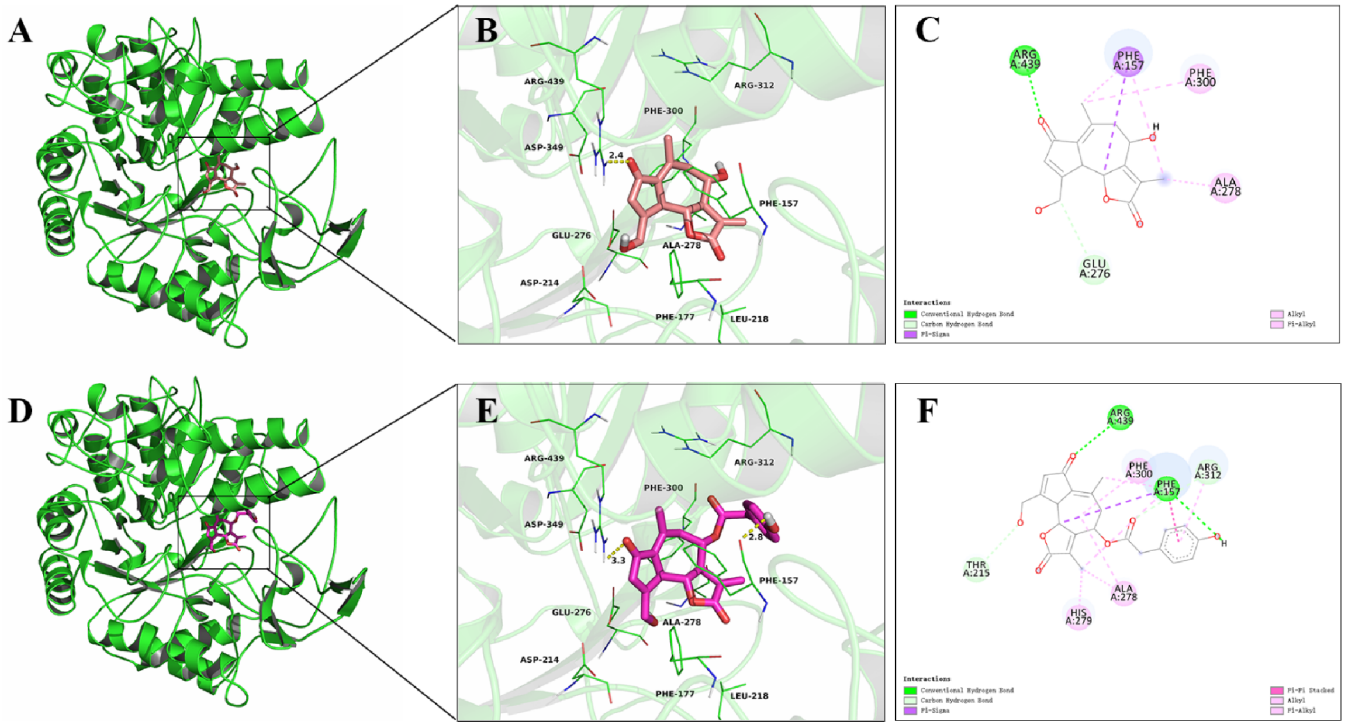

Figure 6. Interaction analysis of lactucin/lactucopicrin with α-glucosidase for optimal energetic ordering results of docking. (A) A molecular docking diagram of lactucin and α-glucosidase and (B) interaction details of the amino acid residues of lactucin and α-glucosidase in an expanded view of the predicted high affinity pocket. (C) Different colored circles and lines represent the types of interactions of amino acid residues with Lactucin, showing a surface view of α-glucosidase with lactucin; (D) molecular docking diagram of lactucopicrin and α-glucosidase; and (E) details of the amino acid residues of lactucopicrin and α-glucosidase in the interaction details, an expanded view of the predicted high-affinity pocket. (F) Circles and lines of different colors represent the types of interactions of amino acid residues with lactucopicrin, demonstrating the surface diagram of α-glucosidase with lactucopicrin.

it is worth mentioning that the Phe-157 residue established hydrogen bonding along with $\pi-\sigma$, $\pi-\pi$ stacking, and alkyl and π−alkyl interactions with lactucopicrin. Furthermore, lactucopicrin forms one additional hydrogen bond with the enzyme compared to lactucin. This extra hydrogen bond interacts with the side chain 2-(4-hydroxyphenyl)acetate group in lactucopicrin. This finding confirms that the additional portion in lactucopicrin enhances its ability to bind more strongly to the enzyme, resulting in a higher enzyme inhibitory activity compared to lactucin.

2.14. Molecular Dynamics Results. The putative binding mechanism between lactucin, lactucopicrin, and α-glucosidase was investigated by molecular docking and molecular dynamics simulations using AutoDock vina 1.1.2 and Amber 14 software package. The binding mechanism of the α-glucosidase−lactucin complex and α-glucosidase−lactucopicrin complex was determined using 40 ns molecular dynamics simulations, building upon the docking results. In order to assess the dynamic stability of the models and validate the sampling approach, we determined the root-mean-square deviation (RMSD) values of the protein backbone throughout the simulation time, depending on the initial structure. These values were then shown in Figure 7a. The simulation resulted in stabilization of the protein structures in all three systems.

The root-mean-square fluctuations (RMSF) of the protein residues in the α-glucosidase−lactucin complex, α-glucosidase−lactucopicrin complex, and free α-glucosidase were computed to assess the flexibility of these residues. The root-mean-square fluctuations (RMSF) of these residues are illustrated in Figure 7b, clearly indicating distinct variations in the flexibility of the binding site of α-glucosidase when lactucin and lactucopicrin are present or absent. The residues in the α-glucosidase binding site that interact with lactucin and lactucopicrin exhibit little flexibility, with a root-mean-square fluctuation (RMSF) of less than 2 Å in comparison to the unbound α-glucosidase. This suggests that these residues become more rigid upon binding to lactucin and lactucopicrin.

The radius of gyration (Rg) is a measure used to assess the compactness of a protein's structure. A lower number suggests a greater protein stability. The gyration radius of lactucopicrin was determined to be smaller than that of free α-glucosidase, whereas the gyration radius of lactucin was found to be higher. A lower Rg value indicates that lactucopicrin effectively coupled to α-glucosidase and formed a very stable system (Figure 7d), resulting in significant inhibitory action. A greater Rg value indicated that the α-glucosidase−lactucin complex had a less compact structure (Figure 7d).

In order to obtain further information regarding the residues next to the binding site and their impact on the overall system, we utilized the MMGBSA approach to compute the electrostatic, van der Waals, solvation, and total contributions of these residues to the binding free energy. The per residue interaction free energies were divided into van der Waals (ΔE_{vdw}), solvation (ΔE_{sol}), electrostatic (ΔE_{ele}), and total contribution (ΔE_{total}). In the combination between α-glucosidase and Lactucin, residue Asp-214 makes a significant electrostatic contribution (ΔE_{ele}) with a ΔE_{ele} value of less than −9.0 kcal/mol (Figure 7e). Upon conducting a thorough examination, it was shown that the residue Asp-214 was in close proximity to the hydroxyl group of lactucin, resulting in the formation of a

https://doi.org/10.1021/acsomega.4c00699
ACS Omega 2024, 9, 19401−19417

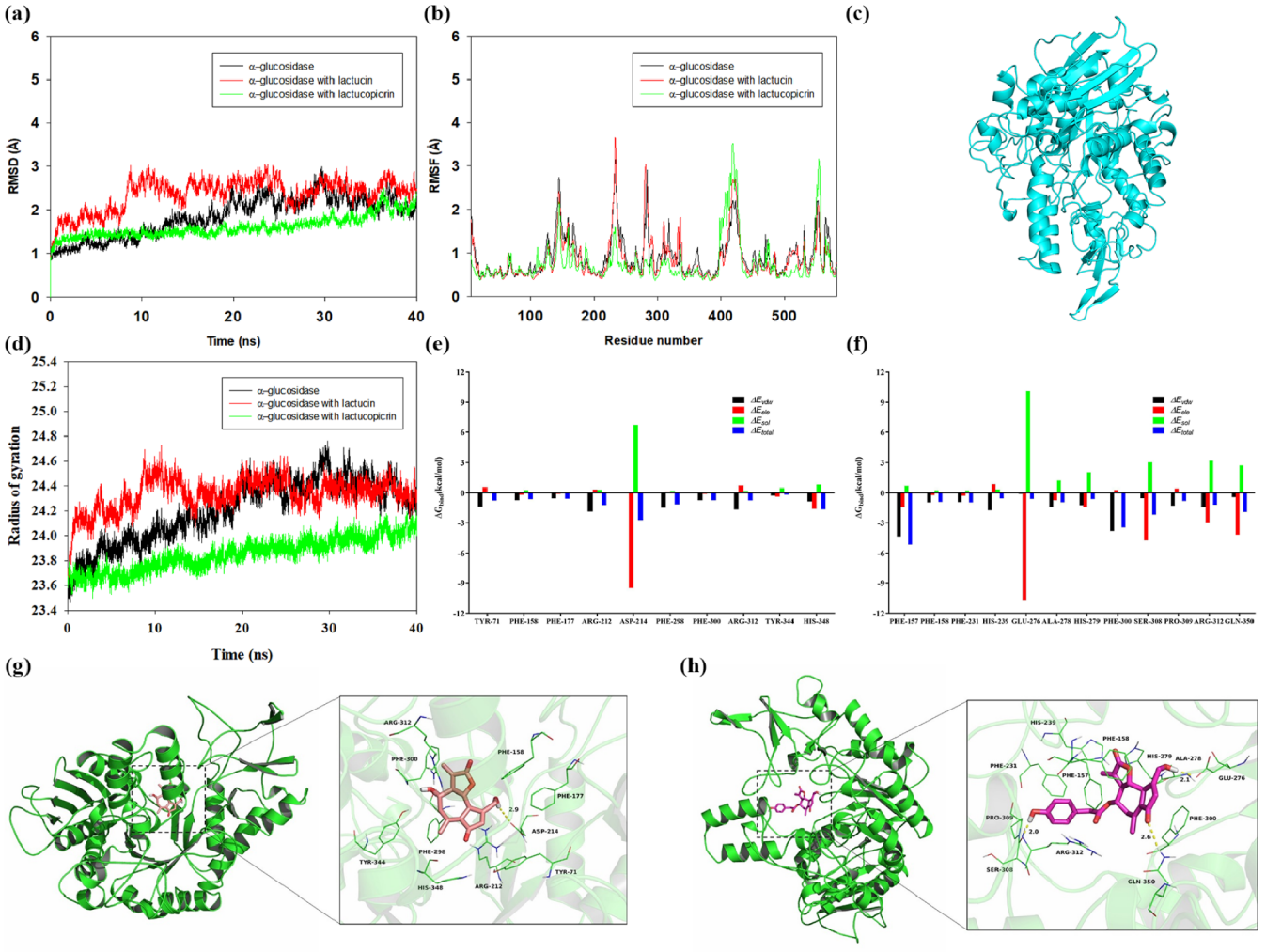

Figure 7. Molecular dynamics of α-glucosidase activity pocket residues lactucin and lactucopicrin. (a) Dynamic simulation of RMSD changes in complex and free protein systems above 20 ns; (b) RMSF values of binding site residues in the free protein and complex systems; (c) homology modeling of the structure of α-glucosidase after homology modeling; (d) radius of gyration of complex and free α-glucosidase systems; molecular dynamics simulation of the complexation of α-glucosidase with lactucin (e) and lactucopicrin (f) decomposition of residue energy contributions during complexation; predicted binding modes of lactucin (g) and lactucopicrin (h) in the predicted α-glucosidase binding pocket obtained by MD simulations.

hydrogen bond interaction. The bond length between them was measured to be 2.9 Å, as depicted in Figure 7g. Furthermore, residues Arg-212 and Arg-312 have a ΔE_{vdw} value of less than −1.5 kcal/mol, indicating a moderate van der Waals contact with the ligand due to their close proximity to lactucin. Primarily, the majority of the energy interactions that have undergone decomposition may be attributed to van der Waals contacts. Specifically, these connections are generally facilitated by hydrophobic interactions, particularly involving amino acids Phe-158, Phe-177, Phe-298, and Phe-300.

In the combination between α-glucosidase and lactucopicrin, residue Glu-276 makes a significant electrostatic contribution (ΔE_{ele}) with a value of less than −10.0 kcal/mol (Figure 7f). Upon conducting a thorough investigation, it was shown that the residue Glu-276 was in close proximity to the hydroxyl group of lactucopicrin, resulting in the formation of a hydrogen bond interaction. The bond length between the two was measured to be 2.1 Å, as depicted in Figure 7h. In addition, residues Ser-308 and Gln-350 make a moderate electrostatic (ΔE_{ele}) contribution, with a ΔE_{ele} value of less than −4.0 kcal/mol (Figure 7f). Thorough research revealed that the residues Ser-308 and Gln-350 were in close proximity to the lactucopicrin compound, generating two hydrogen bond interactions with bond lengths of 2.0 and 2.6 Å, as shown in Figure 7h. Furthermore, residue Phe-157 exhibits a robust van der Waals contact with the ligand due to its close proximity to lactucopicrin, as seen by its ΔE_{vdw} value of < −4.0 kcal/mol. The primary source of the decomposed energy interaction was van der Waals contacts, namely, hydrophobic interactions involving Phe-158, Phe-231, Ala-278, Phe-300, and Pro-309.

The MMGBSA approach was used to calculate the total binding free energy for the α-glucosidase−lactucin complex and the α-glucosidase−lactucopicrin complex. The calculated ΔG_{bind} values were −18.9 kcal/mol for lactucin and −38.2 kcal/mol for lactucopicrin. These results indicate that lactucopicrin exhibited greater activity against the binding site of α-glucosidase compared to lactucin. The remarkable efficacy of lactucopicrin can also be elucidated by the binding manner between α-glucosidase and the chemicals. In comparison to lactucin, the 2-(4-hydroxyphenyl) acetic group of lactucopicrin created an additional hydrogen bond

https://doi.org/10.1021/acsomega.4c00699
ACS Omega 2024, 9, 19401−19417

interaction with α-glucosidase, resulting in lactucopicrin being more active than lactucin (Figure 7g,h).

Overall, the molecular dynamics simulations described above offer a logical explanation for the interactions among lactucin, lactucopicrin, and α-glucosidase. This information is helpful for advancing the development of α-glucosidase inhibitors.

3. CONCLUSIONS

Six α-glucosidase inhibitors were discovered in the *CGB* extract by affinity ultrafiltration combined with UPLC−Q-TOF−MS/MS. These six compounds demonstrated superior inhibitory action compared with acarbose, with lactucin and lactucopicrin displaying the most inhibitory activity. This study showed that the most active components of *CGB*, lactucin and lactucopicrin, exhibited potent inhibitory activities against α-glucosidase. Furthermore, the compounds lactucin and lactucopicrin have the ability to bind with the enzyme, resulting in the formation of novel complexes. This interaction alters the enzyme's secondary structure and microenvironment, ultimately leading to the inhibition of its catalytic activity. We conducted a study to examine the interactions of lactucin and lactucopicrin with α-glucosidase using in vitro activity testing, spectrum analysis, and docking simulation research. The findings demonstrated that lactucopicrin exhibited a robust capacity to suppress α-glucosidase activity and attenuate the fluorescence intensity of α-glucosidase. The spontaneous occurrence of lactucin−α-glucosidase and lactucopicrin−α-glucosidase led to structural alterations in α-glucosidase. The obtained results elucidate the inhibitory activities of the two active components, lactucin and lactucopicrin, on α-glucosidase. Additionally, they offer valuable insights into the variations in inhibitory mechanisms resulting from the structural disparities between lactucin and lactucopicrin.

In this study, we found that although there is only a tiny difference in the structure of lactucin and lactucopicrin, the two compounds have a significant difference in the inhibition of α-glucosidase, and the addition of the 2-(4-hydroxyphenyl) acetic acid group in the structure of lactucopicrin enhances its inhibitory activity on the enzyme. It has also been shown in several studies that the glycosylated compounds will have a lower inhibition rate and a weaker binding ability to the enzyme in comparison to the previous compounds. For example, it has been[47] found that adding a hydroxyl group to the C3′ position of the B-ring in the flavonoid structure increased the inhibitory effect of flavonols against α-glucosidase. On the other hand, attaching two sugar molecules to the C3 position of the C-ring reduced the inhibitory effect of flavonols against α-glucosidase. Additionally, it was observed that the active ingredient of astragalus, Mauritius, had a lower inhibitory activity compared to its predecessor. The inhibitory activity of the active ingredient, isoflavone, found in *Astragalus membranaceus*, was more effective against α-glucosidase compared to its glycoside form, isoflavone-7-O-β-D-glucoside. This is because the addition of glucose glycoside at the 7-position resulted in a decrease in its inhibitory activity against α-glucosidase.[48] Our results showed that among the two compounds, lactucin had one more 2-(4-hydroxyphenyl) acetic acid group structure than lactucin in its structure. The difference in this structure instead enhanced the inhibitory activity of lactucin. It increased the ability of lactucin to bind to enzymes, resulting in different inhibitory kinetic results for the two compounds on enzymes. The fluorescence quenching ability of the enzyme is also different, but the quenching mode is the same. Our results showed that among the two compounds, lactucopicrin had one more 2-(4-hydroxyphenyl) acetic acid group structure than lactucin in its structure. The difference in this structure instead enhanced the inhibitory activity of lactucin. It increased the ability of lactucopicrin to bind to enzymes, resulting in different inhibitory kinetic results of the two compounds on enzymes. The fluorescence quenching ability of the enzyme is also different, but the quenching mode is the same. The present studies on inhibiting α-glucosidase by lactucin and lactucopicrin were well characterized. Nevertheless, these experiments were conducted only in a controlled laboratory setting or with isolated enzymes and artificial substrates. Hence, due to the intricate physiological conditions in living organisms, it is necessary to conduct additional experiments in living mice (by creating diabetic mouse models) in order to investigate the mechanism by which lactucin and lactucopicrin regulate blood glucose. This research will contribute to a better understanding of how *CGB* exerts its hypoglycemic effects. Additionally, this study offers a theoretical foundation for enhancing the antidiabetic effectiveness of lactucopicrin by optimizing its structure.

4. MATERIALS AND METHODS

4.1. Materials and Reagents. *Saccharomyces cerevisiae* α-glucosidase (>100 U/mg), *p*-nitrophenyl-β-D-glucopyranoside (*p*NPG), acarbose (purity >99%), quercetin (purity >99%), 3-O-methylquercetin (purity >99%), chrysin (purity >99%), and isochlorogenic acid B (purity >99%) were purchased from Shanghai Yuanye Biotech Ltd. in China; lactucin (purity >99%) and lactucopicrin (purity >99%) were purchased from Xinjiang Institute of Physics and Chemistry, Chinese Academy of Sciences; Watson's purified water was purchased from Watson's Co., Ltd. in China; *p*-nitrophenol and anhydrous sodium carbonate were purchased from Shanghai McLean Biochemistry Co., Ltd. in China. Methanol, acetonitrile and acetic acid were purchased from Thermo Fisher Co., USA. Amicon Ultra-15 Centrifugal Filters (10 kDa) were purchased from Millipore Co. Ltd. (Bedford, Massachusetts, USA).

The following equipment was used: precision analytical balance LE104E (METTLER-TOLEDO Instruments CO., Ltd., USA); ultrahigh performance liquid chromatography (Waters Corporation, USA); quadrupole time-of-flight mass spectrometry mass spectrometry (Waters Corporation, USA); ultrasonic cleaner KQ5200DE (Kunlun Ultrasonic Instrument Co., Ltd., China); 4 °C low-temperature high-speed centrifuge (Shanghai Lixin Scientific Instrument Co. Ltd., China); full-wavelength enzyme labeling instrument Multiskan GO (Thermo Fisher Scientific); electric thermostat incubator DHP-9082 (Shanghai Yiheng Scientific Instrument Co., Ltd., China); refrigerator (Qingdao Haier Co., Ltd., China); medical refrigerator HYC-310 (Qingdao Haier Special Electric Appliance Co. Ltd., China).

4.2. Preparation of CGB Extracts. The herbs used in this experiment were obtained from the Hotan area, Xinjiang, China; the whole herb of *CGB* was taken, crushed, sieved, and weighed precisely 30 g. The herb was extracted by refluxing with 95% ethanol three times, each time for 3 h according to the material−liquid ratio of 1:13 (m/v), filtered, and the filtrates were combined three times, refluxed, and concentrated, and then dried in a water bath for spare use.

4.3. α-Glucosidase Inhibition Assay. The α-glucosidase inhibitory activity was assessed using an enhanced method for

https://doi.org/10.1021/acsomega.4c00699
ACS Omega 2024, 9, 19401−19417

determination, as described in studies.[31,49] α-Glucosidase has the ability to catalyze the hydrolysis of *p*NPG, resulting in the production of PNP. PNP exhibits its highest absorption at a wavelength of 405 nm in an alkaline environment.The enzyme marker was used to assess the concentration of PNP generated in the reaction. This marker is capable of detecting the inhibitory activity of α-glucosidase in the sample. The enzyme inhibitory activities of the two extracts of hairy chicory were assessed by utilizing *p*NPG as the substrate and acarbose as the positive control. 96-well plates were prepared by adding PBS buffer (total volume of 160 μL), the samples, and an α-glucosidase solution (2 U/mL). The reaction was conducted at 37 °C for 10 min. Subsequently, 0.5 mmol/L of *p*NPG was added and the reaction was incubated for an additional 20 min at 37 °C. This was followed by the addition of 0.0 mmol/L of *p*NPG to each well, and then 0.5 mmol/L of *p*NPG to each well. The reaction was halted by introducing a 0.1 mol/L of Na_2CO_3 solution to each well. The absorbance (OD) at 405 nm was subsequently measured using an enzyme marker. The amount of reagent used in each group of the reaction system is indicated in Table 6. The samples were tested for their inhibitory efficacy against α-glucosidase. The calculation of α-glucosidase inhibition for each sample can be determined using the following formula:

Table 6. Reaction System Dosage (Each Group n = 3)

reagent (μL)	control blank	control	sample blank	sample
PBS	60	40	40	20
α-glucosidase	–	20	–	20
sample	–	–	20	20
*p*NPG	20	20	20	20
Na_2CO_3	80	80	80	80

$$\text{Inhibition Rate} = \frac{\Delta OD_{control} - \Delta OD_{sample}}{\Delta OD_{control}} \times 100\%$$

where $\Delta OD_{control} = OD_{control} - OD_{control\ blank}$ and $\Delta OD_{sample} = OD_{sample} - OD_{sample\ blank}$, in which $OD_{control\ blank}$, $OD_{control}$, OD_{sample}, $OD_{sample\ blank}$ indicate the absorbance values of the control blank group (containing PBS and enzyme), control group (containing only PBS), sample group (containing sample extract, PBS, and enzyme), and sample blank group (containing sample extract and PBS), accordingly.

4.4. Affinity Ultrafiltration Screening of α-Glucosidase Ligands and Identification of Ligands in CGB Extracts. The entire experimental technique is illustrated in Figure 8. The binding rate (AD) was determined using the following calculation:

$$\text{Affinity Degree} = \frac{(A_b - A_c)}{A_a} \times 100\%$$

A_a represents the area of each compound's chromatographic peak in the CGB extract solution before ultrafiltration screening. A_b represents the area of each compound's chromatographic peak that is bound by the active enzyme after affinity interaction. A_c represents the area of each compound's chromatographic peak that is bound by the inactive enzyme.

4.5. α-Glucosidase Inhibition Assay of Screened Ligands. The procedure is identical to the one described in Section 4.3, in which the tested substances were evaluated for their ability to inhibit the enzyme's activity. The extent of inhibition caused by each molecule against α-glucosidase was then compared.

4.6. Kinetics of α-Glucosidase Inhibition. According to the study[50] methodology and with slight modifications, the reaction rate was determined by varying the α-glucosidase concentration (0.2−2.0 U/mL) by setting the substrate *p*NPG concentration to 6.4 mmol/L in the presence of the indicated

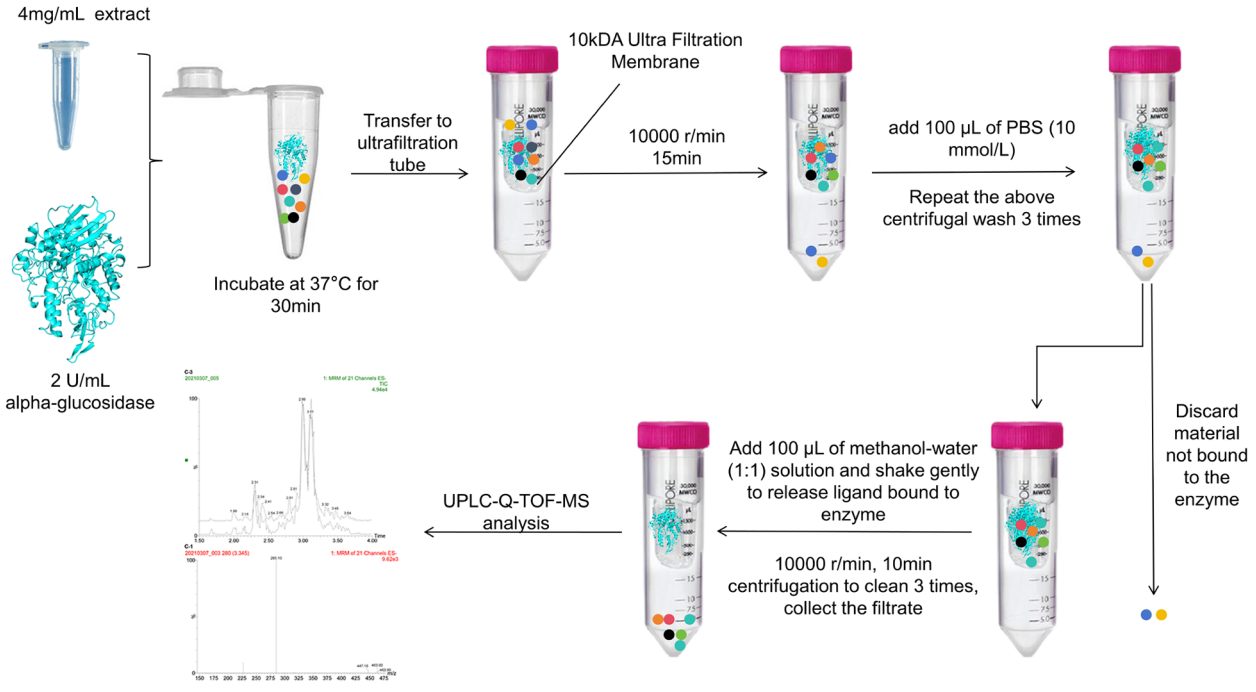

Figure 8. Affinity ultrafiltration-assisted LC−MS/MS analysis.

https://doi.org/10.1021/acsomega.4c00699
ACS Omega 2024, 9, 19401−19417

concentrations of inhibitors, lactucin or lactucopicrin (0, 26.09, and 65.22 μM) inhibitor, to determine its reversibility. The reversibility of the inhibitory activity of lactucin and lactucopicrin against α-glucosidase was assessed by plotting the reaction rate (v) against the concentration of α-glucosidase ([E]) for different concentrations of the inhibitors.[51]

The concentrations of pNPG (1.6, 3.5, 6.4, 9.6, 12.8, and 16.0 mmol/L) at different concentrations of inhibitors were selected to maintain the enzyme concentration at 2 U/mL. The kinetics of enzyme inhibition was further determined. The study focused on examining the inhibition type and kinetic parameters of lactucin and lactucopicrin. This was done by applying a nonlinear regression analysis to the kinetic equation of enzyme inhibition, which took into account the substrate concentration and reaction rate. The inhibitory mechanism can be characterized as a double inverse form,[52] Michaelis–Menten equations in GraphPad Prism 9 Software were utilized to calculate the Michaelis constants (K_m) and maximum reaction rates for different concentrations of lactucin and lactucopicrin (v_{max}).[53]

$$v = (A_2 - A_1)/\Delta T$$

$$\frac{1}{v} = \left(\frac{K_m}{v_{max}}\right)\frac{1}{[S]} + \frac{1}{v_{max}}$$

The following equation describes competitive inhibition:

$$\frac{1}{v} = \left(\frac{K_m}{v_{max}}\right)\left(1 + \frac{[I]}{K_i}\right)\frac{1}{[S]} + \frac{1}{v_{max}}$$

Secondary plots can be constructed as:

$$K_m^{app} = \frac{K_m[I]}{K_i} + K_m$$

The phenomenon of noncompetitive inhibition can be mathematically represented using the following equations:

$$\frac{1}{v} = \left(\frac{K_m}{v_{max}}\right)\left(1 + \frac{[I]}{K_i}\right)\frac{1}{[S]} + \frac{1}{v_{max}}\left(1 + \frac{[I]}{K_i}\right)$$

Secondary plots can be constructed as:

$$\frac{1}{v_{max}^{app}} = \frac{[I]}{(v_{max}K_i)} + \frac{1}{v_{max}}$$

where v is the enzyme reaction rate in the absence and presence of α-glucosidase and K_i and K_m are the inhibition constant and Michaelis–Menten constant, respectively. Their values can be obtained from the above equation. [I] and [S] are the concentrations of the inhibitor and substrate, respectively. K_m^{app} and v_{max}^{app} are the apparent Michaelis–Menten constant and apparent reaction rate, respectively.[25]

4.7. Fluorescence Spectral Analysis. Various concentrations of lactucin (0–65.22 μM) and lactucopicrin (0–65.22 μM) were titrated into a fixed concentration of α-glucosidase (2 U/mL) solution and incubated at two different temperatures, 298 and 310 K, for 30 min. Samples were then transferred to a cuvette (1 cm), and fluorescence spectra were determined using an RF-6000 fluorescence spectrophotometer to determine the fluorescence spectra. The excitation wavelength was 280 nm, the emission wavelength was 300–500 nm, and the slit width was 2.5 nm. All spectra were subtracted from the background fluorescence of the PBS solution.[29]

Synchronized fluorescence spectra of α-glucosidase were measured in the range of 260–320 nm at 298 K by setting the interval $\Delta\lambda$ ($\Delta\lambda=\lambda_{em}-\lambda_{ex}$) between excitation and emission wavelengths to 15 and 60 nm. This spectrum showed the changes in tyrosine (Tyr) and tryptophan (Trp) residue microenvironments of α-glucosidase enzyme before and after incorporating small molecules, respectively.

3D fluorescence spectra were likewise measured on a fluorescence spectrophotometer. The excitation wavelength range was 210–420 nm, and the emission wavelength range was 210–420 nm. The 3D fluorescence spectra of α-glucosidase (2 U/mL) were determined in the absence and presence of the inhibitor.

4.8. FT-IR Analysis. Three samples (α-glucosidase solution, lactucin–α-glucosidase solution, and lactucopicrin–α-glucosidase solution) were examined using a Fourier transform infrared spectrometer (FT-IR) in the range 1800–1500 cm^{-1} at room temperature. Lactucin–α-glucosidase and lactucopicrin–α-glucosidase samples should be preprepared. The compounds are mixed with the enzyme solution and left to react fully. In the three samples, the concentration of α-glucosidase was 2 U/ml, and the concentration of lactucin and lactucopicrin was 65.22 μM.[54,55]

4.9. Circular Dichroism (CD). Far-ultraviolet (200–260 nm) CD measurements were performed using the method described above to reveal conformational changes in the enzyme, and CD spectra of α-glucosidase with and without the inhibitors (lactucin and lactucopicrin) were recorded with a CD spectrometer. The CD spectral data of the enzymes with and without inhibitors were analyzed under the same conditions, minus the PBS, using the online SELCON3 program. α-Glucosidase (2U/mL) was mixed and reacted with lactucin (65.22 μM) and lactucopicrin (65.22 μM), for 30 min at 37 °C, and the reaction solutions were scanned in the range of 200–260 nm. All results were analyzed on a professional website (http:// dichroweb.cryst.bbk.ac.uk/html/home.shtml).[56]

4.10. UV Analysis. The UV absorption spectra of α-glucosidase in the presence and absence of lactucin and lactucopicrin were recorded by using a UV spectrophotometer to analyze the effect of inhibitors on the structure of the protein. According to the study[39] method, the concentration of α-glucosidase was 2 U/mL, and the concentration of lactucin and lactucopicrin was set at 65.22 μM. The two samples were mixed with the enzyme and incubated for 30 min, and the spectra were measured in the 200–500 nm range. The UV absorbance values of the corresponding concentrations of lactucin and lactucopicrin were deducted.

4.11. Molecular Docking. An investigation was conducted utilizing molecular docking to evaluate the binding mechanism between the chemicals and *Saccharomyces cerevisiae* α-glucosidase. Autodock vina 1.1.2. was used for this purpose.[57] The α-glucosidase's three-dimensional (3D) structure was constructed using SWISS-MODEL, which is a completely automated service for homology-modeling of protein structures. The compound's 3D structure was shown using ChemBioDraw Ultra 14.0 and ChemBio 3D Ultra 14.0 software. The AutoDockTools 1.5.6 package generated the docking input files.[58,59] The process of modeling α-glucosidase is referenced in article.[60] The search grid for the α-glucosidase enzyme was determined to have a center position of x: −20.047, y: −8.307, and z: −22.315, with dimensions of x: 15, y: 15, and z: 15. The ligand structures were created for docking

https://doi.org/10.1021/acsomega.4c00699
ACS Omega 2024, 9, 19401–19417

by combining nonpolar hydrogen atoms and establishing definitions. To enhance the precision of docking, the exhaustiveness parameter was adjusted to 16. If not specified, the default parameters were employed for Vina docking. Subsequently, molecular dynamics (MD) research was conducted to reassess the docking outcome.

4.12. Molecular Dynamics (MD). The MD simulations of the selected docked pose were conducted using the Amber 14[61−63] and AmberTools 15 software packages. The molecule was initially synthesized using ACPYPE,[64] a tool that relies on ANTECHAMBER[65,66] for automatically creating topologies and parameters in various formats for different molecular mechanics programs. This tool also calculates the partial charges. The ligand was prepared using the "leaprc.gaff" (generalized amber force field), while the receptor was prepared using "leaprc.ff14SB." The system was enclosed into a rectangular box, with a boundary of 10.0 Å, using the "SolvateOct" command. The solute atoms were positioned at a minimum distance from each other within the box, which was filled with TIP3P water. The solvated complex was equilibrated in a series of steps. First, a short minimization was performed using both the steepest descent and conjugate gradient methods with 500 steps for each. Next, the system was heated for 500 ps. Finally, a density equilibration was carried out for 50 ps, with weak restraints applied. This entire process was accelerated using the GPU (NVIDIA Tesla K20c) accelerated PMEMD (Particle Mesh Ewald Molecular Dynamics) module. Finally, a total of 40 ns of molecular dynamics simulations were conducted. The molecular dynamics simulations were conducted using a Dell Precision T5500 workstation.

4.12.1. Binding Free Energy and Energy Decomposition per Residue Calculations. The ΔG_{bind} values in kcal/mol were computed by using the Molecular Mechanics/Generalized Born Surface Area (MM/GBSA) method, which was implemented in AmberTools 15. Furthermore, the binding free energy was analyzed by breaking it down on a per-residue basis in order to determine the specific protein residues that play a crucial role in the process of ligand binding. The binding free energy of each complex was determined using the MM/GBSA method.

$$\Delta G_{bind} = G_{complex} - G_{protein} - G_{ligand}$$

Where ΔG_{bind} is the binding free energy and $G_{complex}$, $G_{protein}$, and G_{ligand} are the free energies of complex, protein, and ligand, respectively.

4.13. Statistical Analysis. All data repeated three times are expressed as the mean ± standard deviation. Nonlinear regression was performed using GraphPad Prism 9 (GraphPad Software Inc., San Diego, CA, USA) so that the 50% inhibitory concentration in the enzyme activity assay could be calculated (IC_{50}).

■ ASSOCIATED CONTENT

Supporting Information

The Supporting Information is available free of charge at https://pubs.acs.org/doi/10.1021/acsomega.4c00699.

Additional experimental details, materials, and methods, including photographs of experimental setup (PDF)

■ AUTHOR INFORMATION

Corresponding Author

Xiaoli Ma − *School of Pharmacy, Xin Jiang Medical University, Urumqi 830054, China;* orcid.org/0000-0002-3972-8109; Email: mxl108@sohu.com, xiaoli_ma@xjmu.edu.cn

Authors

Adalaiti Abudurexiti − *School of Pharmacy, Xin Jiang Medical University, Urumqi 830054, China*

Abliz Abdurahman − *School of Pharmacy, Xin Jiang Medical University, Urumqi 830054, China*

Rui Zhang − *School of Pharmacy, Xin Jiang Medical University, Urumqi 830054, China*

Yewei Zhong − *School of Pharmacy, Xin Jiang Medical University, Urumqi 830054, China*

Yi Lei − *School of Pharmacy, Xin Jiang Medical University, Urumqi 830054, China*

Shuwen Qi − *School of Pharmacy, Xin Jiang Medical University, Urumqi 830054, China*

Wenhui Hou − *School of Pharmacy, Xin Jiang Medical University, Urumqi 830054, China*

Complete contact information is available at: https://pubs.acs.org/10.1021/acsomega.4c00699

Author Contributions

⊥A.A. and A.A. contributed equally. X.M. and A.A. came up with the idea for the study and designed it. A.A., A.A., R.Z., Y.Z., Y.L., S.Q., and W.H. conducted the experiments. X.M. provided guidance for the study. A.A. analyzed the data and wrote the manuscript. All authors reviewed and approved the manuscript. The data were exclusively developed in-house, without the involvement of any external sources. All authors have unanimously agreed to assume accountability for all parts of the work. Guarantee the honesty and precision of the work.

Notes

The authors declare no competing financial interest.

■ ACKNOWLEDGMENTS

The authors are thankful to the Major science and technology projects of Xinjiang Uygur Autonomous Region of China (No. 2022A03007-3) and (No. 2022A0319-3); and the Tianshan Talent Youth Top Talent Project of Xinjiang Uygur Autonomous Region of China (No. 2022TSYCCX0104) for funding support.

■ REFERENCES

(1) Wu, X.; Ding, H.; Hu, X.; Pan, J.; Liao, Y.; Gong, D.; Zhang, G. Exploring inhibitory mechanism of gallocatechin gallate on a-amylase and a-glucosidase relevant to postprandial hyperglycemia. *J. Funct. Foods* **2018**, *48*, 200−209.

(2) Lu, X.; Zhang, M.; Qiu, Y.; Liu, X.; Wang, C.; Chen, J.; Zhang, H.; Wei, B.; Yu, Y.; Ying, Y.; Hong, K.; Wang, H. α-Glucosidase Inhibitors from Two Mangrove-Derived Actinomycetes. *Molecules* **2023**, *28*, 9.

(3) Yang, J.; Li, H.; Wang, X.; Zhang, C.; Feng, G.; Peng, X. Inhibition Mechanism of α-Amylase/α-Glucosidase by Silibinin, its Synergism with Acarbose, and the Effect of Milk Proteins. *J. Agric. Food Chem.* **2021**, *69* (36), 10515−10526.

(4) Sun, H.; Wang, D.; Song, X.; Zhang, Y.; Ding, W.; Peng, X.; Zhang, X.; Li, Y.; Ma, Y.; Wang, R.; Yu, P. Natural Prenylchalconaringenins and Prenylnaringenins as Antidiabetic Agents: α-Glucosidase and α-Amylase Inhibition and in Vivo Antihyperglycemic and Antihyperlipidemic Effects. *J. Agric. Food Chem.* **2017**, *65* (8), 1574−1581.

(5) Zeng, L.; Zhang, G.; Lin, S.; Gong, D. Inhibitory Mechanism of Apigenin on alpha-Glucosidase and Synergy Analysis of Flavonoids. *J. Agric. Food Chem.* **2016**, *64* (37), 6939−6949.

(6) Tran, T. D.; Bui, T. Q.; Le, T. A.; Nguyen, M. T.; Hai, N. T. T.; Pham, N. H.; Phan, M. N.; Healy, P. C.; Pham, N. B.; Quinn, R. J.; Quy, P. T.; Triet, N. T.; Nguyen, H. N.; Le, N. H.; Phung, T. V.; Nhung, N. T. A. Styracifoline from the Vietnamese Plant Desmodium styracifolium: A Potential Inhibitor of Diabetes-Related and Thrombosis-Based Proteins. *ACS Omega* **2021**, *6* (36), 23211−23221.
(7) Zhao, X.; Tao, J.; Zhang, T.; Jiang, S.; Wei, W.; Han, H.; Shao, Y.; Zhou, G.; Yue, H. Resveratroloside Alleviates Postprandial Hyperglycemia in Diabetic Mice by Competitively Inhibiting α-Glucosidase. *J. Agric. Food Chem.* **2019**, *67* (10), 2886−2893.
(8) Gu, S.; Shi, J.; Tang, Z.; Sawhney, M.; Hu, H.; Shi, L.; Fonseca, V.; Dong, H. Comparison of glucose lowering effect of metformin and acarbose in type 2 diabetes mellitus: A meta-analysis. *PloS One* **2015**, *10* (5), No. e0126704.
(9) Valdés, M.; Calzada, F.; Mendieta-Wejebe, J. E.; Merlín-Lucas, V.; Velázquez, C.; Barbosa, E. Antihyperglycemic Effects of Annona diversifolia Safford and Its Acyclic Terpenoids: α-Glucosidase and Selective SGLT1 Inhibitiors. *Molecules* **2020**, *25* (15), 3361.
(10) McDougall, G. J.; Shpiro, F.; Dobson, P.; Smith, P.; Blake, A.; Stewart, D. Different polyphenolic components of soft fruits inhibit alpha-amylase and alpha-glucosidase. *J. Agric. Food Chem.* **2005**, *53* (7), 2760−2766.
(11) Li, D.-Q.; Qian, Z.-M.; Li, S.-P. Inhibition of Three Selected Beverage Extracts on alpha-Glucosidase and Rapid Identification of their Active Compounds Using HPLC-DAD-MS/MS and Biochemical Detection. *J. Agric. Food Chem.* **2010**, *58* (11), 6608−6613.
(12) Carazzone, C.; Mascherpa, D.; Gazzani, G.; Papetti, A. Identification of phenolic constituents in red chicory salads (Cichorium intybus) by high-performance liquid chromatography with diode array detection and electrospray ionisation tandem mass spectrometry. *Food Chem.* **2013**, *138* (2−3), 1062−1071.
(13) Tong, J.; Ma, B.; Ge, L.; Mo, Q.; Zhou, G.; He, J.; Wang, Y. Dicaffeoylquinic Acid-Enriched Fraction of Cichorium glandulosum Seeds Attenuates Experimental Type 1 Diabetes via Multipathway Protection. *J. Agric. Food Chem.* **2015**, *63* (50), 10791−10802.
(14) Atta Ur, R.; Zareen, S.; Choudhary, M. I.; Akhtar, M. N.; Khan, S. N. alpha-glucosidase inhibitory activity of triterpenoids from Cichorium intybus. *J. Nat. Prod.* **2008**, *71* (5), 910−913.
(15) Dalar, A.; Konczak, I. Cichorium intybus from Eastern Anatolia: Phenolic composition, antioxidant and enzyme inhibitory activities. *Ind. Crops Prod.* **2014**, *60*, 79−85.
(16) Yao, X.; Zhu, L.; Chen, Y.; Tian, J.; Wang, Y. In vivo and in vitro antioxidant activity and alpha-glucosidase, alpha-amylase inhibitory effects of flavonoids from Cichorium glandulosum seeds. *Food Chem.* **2013**, *139* (1−4), 59−66.
(17) Chen, H.; Qin, H.; Long, F.; Yu, W.; Wang, Y.; Chen, L.; Li, Q.; Chen, W.; Qin, D.; Han, B. Screening of High-Affinity alpha-Glucosidase Inhibitors from Cichorium Glandulosum Boiss. et Hout Seed Based on Ultrafiltration Liquid Chromatography-Mass Spectrometry and Molecular Docking. *Chin. J. Anal. Chem.* **2017**, *45* (6), 889−897.
(18) Upur, H.; Amat, N.; Blazekovic, B.; Talip, A. Protective effect of Cichorium glandulosum root extract on carbon tetrachloride-induced and galactosamine-induced hepatotoxicity in mice. *Food Chem. Toxicol.* **2009**, *47* (8), 2022−2030.
(19) Chen, P. X.; Tang, Y.; Zhang, B.; Liu, R.; Marcone, M. F.; Li, X.; Tsao, R. 5-hydroxymethyl-2-furfural and derivatives formed during acid hydrolysis of conjugated and bound phenolics in plant foods and the effects on phenolic content and antioxidant capacity. *J. Agric. Food Chem.* **2014**, *62* (20), 4754−4761.
(20) Wang, J.; Liu, S.; Ma, B.; Chen, L.; Song, F.; Liu, Z.; Liu, C. M. Rapid screening and detection of XOD inhibitors from S. tamariscina by ultrafiltration LC-PDA-ESI-MS combined with HPCCC. *Anal. Bioanal. Chem.* **2014**, *406* (28), 7379−7387.
(21) Ji, T.; Li, J.; Su, S.-L.; Zhu, Z.-H.; Guo, S.; Qian, D.-W.; Duan, J.-A. Identification and Determination of the Polyhydroxylated Alkaloids Compounds with α-Glucosidase Inhibitor Activity in Mulberry Leaves of Different Origins. *Molecules* **2016**, *21* (2), 206.
(22) Li, J.; Yang, P.; Yang, Q.; Gong, X.; Ma, H.; Dang, K.; Chen, G.; Gao, X.; Feng, B. Analysis of Flavonoid Metabolites in Buckwheat Leaves Using UPLC-ESI-MS/MS. *Molecules* **2019**, *24* (7), 1310.
(23) Li, S.; Wang, R.; Hu, X.; Li, C.; Wang, L. Bio-affinity ultrafiltration combined with HPLC-ESI-qTOF-MS/MS for screening potential α-glucosidase inhibitors from Cerasus humilis (Bge.) Sok. leaf-tea and in silico analysis. *Food Chem.* **2022**, *373*, 131528.
(24) Wang, L.; Liu, Y.; Luo, Y.; Huang, K.; Wu, Z. Quickly Screening for Potential alpha-Glucosidase Inhibitors from Guava Leaves Tea by Bioaffinity Ultrafiltration Coupled with HPLC-ESI-TOF/MS Method. *J. Agric. Food Chem.* **2018**, *66* (6), 1576−1582.
(25) Rehman, N. U.; Halim, S. A.; Al-Azri, M.; Khan, M.; Khan, A.; Rafiq, K.; Al-Rawahi, A.; Csuk, R.; Al-Harrasi, A. Triterpenic Acids as Non-Competitive α-Glucosidase Inhibitors from Boswellia elongata with Structure-Activity Relationship: In Vitro and In Silico Studies. *Biomolecules* **2020**, *10* (5), 751.
(26) Zhao, L.; Wen, L.; Lu, Q.; Liu, R. Interaction mechanism between alpha-glucosidase and A-type trimer procyanidin revealed by integrated spectroscopic analysis techniques. *Int. J. Biol. Macromol.* **2020**, *143*, 173−180.
(27) Liu, J.-L.; Kong, Y.-C.; Miao, J.-Y.; Mei, X.-Y.; Wu, S.-Y.; Yan, Y.-C.; Cao, X.-Y. Spectroscopy and molecular docking analysis reveal structural specificity of flavonoids in the inhibition of alpha-glucosidase activity. *Int. J. Biol. Macromol.* **2020**, *152*, 981−989.
(28) Rao, H.; Qi, W.; Su, R.; He, Z.; Peng, X. Mechanistic and conformational studies on the interaction of human serum albumin with rhodamine B by NMR, spectroscopic and molecular modeling methods. *J. Mol. Liq.* **2020**, *316*, 113889.
(29) Ding, H.; Wu, X.; Pan, J.; Hu, X.; Gong, D.; Zhang, G. New Insights into the Inhibition Mechanism of Betulinic Acid on alpha-Glucosidase. *J. Agric. Food Chem.* **2018**, *66* (27), 7065−7075.
(30) Liu, D.; Cao, X.; Kong, Y.; Mu, T.; Liu, J. Inhibitory mechanism of sinensetin on α-glucosidase and non-enzymatic glycation: Insights from spectroscopy and molecular docking analyses. *Int. J. Biol. Macromol.* **2021**, *166*, 259−267.
(31) Han, L.; Fang, C.; Zhu, R.; Peng, Q.; Li, D.; Wang, M. Inhibitory effect of phloretin on α-glucosidase: Kinetics, interaction mechanism and molecular docking. *Int. J. Biol. Macromol.* **2017**, *95*, 520−527.
(32) Ni, M.; Hu, X.; Gong, D.; Zhang, G. Inhibitory mechanism of vitexin on α-glucosidase and its synergy with acarbose. *Food Hydrocolloids* **2020**, *105*, 105824.
(33) Chen, Z.; Chen, Y.; Xue, Z.; Gao, X.; Jia, Y.; Wang, Y.; Lu, Y.; Zhang, J.; Zhang, M.; Chen, H. Insight into the inactivation mechanism of soybean Bowman-Birk trypsin inhibitor (BBTI) induced by epigallocatechin gallate and epigallocatechin: Fluorescence, thermodynamics and docking studies. *Food Chem.* **2020**, *303*, 125380.
(34) Hou, Z.-W.; Chen, C.-H.; Ke, J.-P.; Zhang, Y.-Y.; Qi, Y.; Liu, S.-Y.; Yang, Z.; Ning, J.-M.; Bao, G.-H. α-Glucosidase Inhibitory Activities and the Interaction Mechanism of Novel Spiro-Flavoalkaloids from YingDe Green Tea. *J. Agric. Food Chem.* **2022**, *70* (1), 136−148.
(35) Javaheri-Ghezeldizaj, F.; Soleymani, J.; Kashanian, S.; Dolatabadi, J. E. N.; Dehghan, P. Multi-spectroscopic, thermodynamic and molecular dockimg insights into interaction of bovine serum albumin with calcium lactate. *Microchem. J.* **2020**, *154*, 104580.
(36) Dai, T.; Chen, J.; McClements, D. J.; Li, T.; Liu, C. Investigation the interaction between procyanidin dimer and alpha-glucosidase: Spectroscopic analyses and molecular docking simulation. *Int. J. Biol. Macromol.* **2019**, *130*, 315−322.
(37) Wang, S.; Xie, X.; Zhang, L.; Hu, Y.-M.; Wang, H.; Tu, Z.-C. Inhibition mechanism of α-glucosidase inhibitors screened from Artemisia selengensis Turcz root. *Ind. Crops Prod.* **2020**, *143*, 111941.
(38) Yu, Y.; Ding, X.; Ding, Z.; Wang, Y.; Song, Y. Fluorescence spectroscopy and molecular docking analysis of the binding of Lactobacillus acidophilus GIM1.208 β-glucosidase with quercetin glycosides. *Enzyme Microb. Technol.* **2021**, *146*, 109761.

https://doi.org/10.1021/acsomega.4c00699
ACS Omega 2024, 9, 19401−19417

(39) Yang, J.; Wang, X.; Zhang, C.; Ma, L.; Wei, T.; Zhao, Y.; Peng, X. Comparative study of inhibition mechanisms of structurally different flavonoid compounds on α-glucosidase and synergistic effect with acarbose. *Food Chem.* **2021**, *347*, 129056.
(40) Zheng, Y.; Tian, J.; Yang, W.; Chen, S.; Liu, D.; Fang, H.; Zhang, H.; Ye, X. Inhibition mechanism of ferulic acid against α-amylase and α-glucosidase. *Food Chem.* **2020**, *317*, 126346.
(41) Shi, J. H.; Pan, D. Q.; Wang, X. X.; Liu, T. T.; Jiang, M.; Wang, Q. Characterizing the binding interaction between antimalarial artemether (AMT) and bovine serum albumin (BSA): Spectroscopic and molecular docking methods. *J. Photochem. Photobiol., B* **2016**, *162*, 14−23.
(42) Tang, H.; Huang, L.; Sun, C.; Zhao, D. Exploring the structure-activity relationship and interaction mechanism of flavonoids and α-glucosidase based on experimental analysis and molecular docking studies. *Food Funct.* **2020**, *11* (4), 3332−3350.
(43) Feroz, S. R.; Mohamad, S. B.; Bujang, N.; Malek, S. N. A.; Tayyab, S. Multispectroscopic and Molecular Modeling Approach To Investigate the Interaction of Flavokawain B with Human Serum Albumin. *J. Agric. Food Chem.* **2012**, *60* (23), 5899−5908.
(44) Liu, Y.; Zhu, J.; Yu, J.; Chen, X.; Zhang, S.; Cai, Y.; Li, L. A new functionality study of vanillin as the inhibitor for α-glucosidase and its inhibition kinetic mechanism. *Food Chem.* **2021**, *353*, 129448.
(45) Pan, X.; Qin, P.; Liu, R.; Wang, J. Characterizing the Interaction between Tartrazine and Two Serum Albumins by a Hybrid Spectroscopic Approach. *J. Agric. Food Chem.* **2011**, *59* (12), 6650−6656.
(46) Liu, W.; Li, H.; Wen, Y.; Liu, Y.; Wang, J.; Sun, B. Molecular Mechanism for the alpha-Glucosidase Inhibitory Effect of Wheat Germ Peptides. *J. Agric. Food Chem.* **2021**, *69* (50), 15231−15239.
(47) Qin, Y.; Chen, X.; Xu, F.; Gu, C.; Zhu, K.; Zhang, Y.; Wu, G.; Wang, P.; Tan, L. Effects of hydroxylation at C3′ on the B ring and diglycosylation at C3 on the C ring on flavonols inhibition of α-glucosidase activity. *Food Chem.* **2023**, *406*, 135057.
(48) Han, L.; Song, J.; Yan, C.; Wang, C.; Wang, L.; Li, W.; Du, Y.; Li, Q.; Liang, T. Inhibitory activity and mechanism of calycosin and calycosin-7-O-β-D-glucoside on α-glucosidase: Spectroscopic and molecular docking analyses. *Process Biochem.* **2022**, *118*, 227−235.
(49) Liu, Y.; Zhou, X.; Zhou, D.; Jian, Y.; Jia, J.; Ge, F. Isolation of Chalcomoracin as a Potential α-Glycosidase Inhibitor from Mulberry Leaves and its Binding Mechanism. *Molecules* **2022**, *27* (18), 5742.
(50) Xie, L.; Zhang, T.; Karrar, E.; Zheng, L.; Xie, D.; Jin, J.; Chang, M.; Wang, X.; Jin, Q. Insights into an α-Glucosidase Inhibitory Profile of 4,4-Dimethylsterols by Multispectral Techniques and Molecular Docking. *J. Agric. Food Chem.* **2021**, *69* (50), 15252−15260.
(51) Dong, Q.; Hu, N.; Yue, H.; Wang, H. Inhibitory Activity and Mechanism Investigation of Hypericin as a Novel α-Glucosidase Inhibitor. *Molecules* **2021**, *26* (15), 4566.
(52) Copeland, R. A. Evaluation of enzyme inhibitors in drug discovery. A guide for medicinal chemists and pharmacologists. *Methods Biochem. Anal.* **2005**, *46*, 1−265.
(53) Wang, Y.; Zhang, G.; Yan, J.; Gong, D. Inhibitory effect of morin on tyrosinase: Insights from spectroscopic and molecular docking studies. *Food Chem.* **2014**, *163*, 226−233.
(54) Gupta, R. Letter to the editor in response to article: ″Clinical considerations for patients with diabetes in times of COVID-19 epidemic. *Diabetes Metab. Syndr.* **2020**, *14* (4), 365−365.
(55) Ma, C.; Zhang, J.; Yang, S.; Hua, Y.; Su, J.; Shang, Y.; Wang, Z.; Feng, K.; Zhang, J.; Yang, X.; Zhang, H.; Mao, J.; Fan, G. Astragalus Flavone Ameliorates Atherosclerosis and Hepatic Steatosis Via Inhibiting Lipid-Disorder and Inflammation in apoE−/− Mice. *Front. Pharmacol.* **2020**, *11*, 610550.
(56) Sreerama, N.; Woody, R. W. Estimation of protein secondary structure from circular dichroism spectra: Comparison of CONTIN, SELCON, and CDSSTR methods with an expanded reference set. *Anal. Biochem.* **2000**, *287* (2), 252−260.
(57) Trott, O.; Olson, A. J. Software News and Update AutoDock Vina: Improving the Speed and Accuracy of Docking with a New Scoring Function, Efficient Optimization, and Multithreading. *J. Comput. Chem.* **2010**, *31* (2), 455−461.
(58) Sanner, M. F. Python: A programming language for software integration and development. *J. Mol. Graphics Modell.* **1999**, *17* (1), 57−61.
(59) Morris, G. M.; Huey, R.; Lindstrom, W.; Sanner, M. F.; Belew, R. K.; Goodsell, D. S.; Olson, A. J. AutoDock4 and AutoDockTools4: Automated Docking with Selective Receptor Flexibility. *J. Comput. Chem.* **2009**, *30* (16), 2785−2791.
(60) Wang, G.; Peng, Z.; Wang, J.; Li, X.; Li, J. Synthesis, in vitro evaluation and molecular docking studies of novel triazine-triazole derivatives as potential α-glucosidase inhibitors. *Eur. J. Med. Chem.* **2017**, *125*, 423−429.
(61) Goetz, A. W.; Williamson, M. J.; Xu, D.; Poole, D.; Le Grand, S.; Walker, R. C. Routine Microsecond Molecular Dynamics Simulations with AMBER on GPUs. 1. Generalized Born. *J. Chem. Theory Comput.* **2012**, *8* (5), 1542−1555.
(62) Pierce, L. C. T.; Salomon-Ferrer, R.; de Oliveira, C. A. F.; McCammon, J. A.; Walker, R. C. Routine Access to Millisecond Time Scale Events with Accelerated Molecular Dynamics. *J. Chem. Theory Comput.* **2012**, *8* (9), 2997−3002.
(63) Salomon-Ferrer, R.; Goetz, A. W.; Poole, D.; Le Grand, S.; Walker, R. C. Routine Microsecond Molecular Dynamics Simulations with AMBER on GPUs. 2. Explicit Solvent Particle Mesh Ewald. *J. Chem. Theory Comput.* **2013**, *9* (9), 3878−3888.
(64) Sousa da Silva, A. W.; Vranken, W. F. ACPYPE - AnteChamber PYthon Parser interfacE. *BMC Res. Notes* **2012**, *5* (1), 367−367.
(65) Wang, J. M.; Wolf, R. M.; Caldwell, J. W.; Kollman, P. A.; Case, D. A. Development and testing of a general amber force field (vol 25, pg 1157, 2004). *J. Comput. Chem.* **2005**, *26* (1), 114−114.
(66) Wang, J.; Wang, W.; Kollman, P. A.; Case, D. A. Automatic atom type and bond type perception in molecular mechanical calculations. *J. Mol. Graphics Modell.* **2006**, *25* (2), 247−260.

https://doi.org/10.1021/acsomega.4c00699
ACS Omega 2024, 9, 19401−19417